OXFORD

Journal of Petrology, 2024, **65**, egae023
https://doi.org/10.1093/petrology/egae023
Advance access publication date 12 March 2024
Original Manuscript

Tectonic and Crustal Processes Drive Multi-Million Year Arc Magma Evolution Leading up to Porphyry Copper Deposit Formation in Central Chile

Simon J. E. Large[1], Chetan L. Nathwani[1,2,*], Jamie J. Wilkinson[1,2], Thomas R. Knott[3], Simon R. Tapster[4] and Yannick Buret[1]

[1]London Centre for Ore Deposits and Exploration (LODE), Natural History Museum, Cromwell Road, South Kensington, London SW7 5BD, UK
[2]Department of Earth Science and Engineering, Imperial College London, Exhibition Road, South Kensington Campus, London SW7 2AZ, UK
[3]Centre for Sustainable Resource Extraction, University of Leicester, University Road, Leicester LE1 7RH, United Kingdom
[4]Geochronology and Tracers Facility, British Geological Survey, Keyworth, Nottingham, NG12 5GG UK
*Corresponding author. Present address: Department of Earth Sciences, Institute of Geochemistry and Petrology, ETH Zürich, Clausiusstrasse 25, 8092, Zürich, Switzerland. Telephone: +41 44 632 36 77; E-mail: chetan.nathwani@erdw.ethz.ch

Subduction zone magmatism is a major control of volcanism, the generation of modern continental crust and the formation of economically important porphyry Cu–(Mo–Au) deposits. Reading the magmatic record of individual arc segments and constraining the rates of magmatic changes are critical in order to fully understand and quantify the processes that drive magma evolution in subduction settings during arc growth. This study focuses on the San Francisco Batholith and the Rio Blanco-Los Bronces porphyry deposit cluster in central Chile, which provides an igneous rock record over ~13.5 Myr of arc evolution. We use whole-rock geochemistry, zircon geochronology and Hf isotope geochemistry to track changes in the crustal magmatic system of this arc segment during crustal thickening and porphyry Cu deposit formation. By combining the analytical dataset with Monte Carlo fractional crystallisation and assimilation fractional crystallisation modelling, we test a model for significant crustal involvement during magma evolution. Systematic and continuous increases in Dy/Yb, La/Yb, V/Sc and Sr/Y in the magmas over time indicate a transition in the main fractionation assemblage from plagioclase-dominated to amphibole-dominated that reflects deeper crystallisation and/or a higher meltwater content. Concomitant decreases in ϵHf and Th/La as well as increasing Ba/Th are best explained by assimilation of progressively deeper crustal lithologies from low (Chilenia) to high Ba/Th (Cuyania) basement terranes. Our study highlights that an increasingly hydrous magma and a deepening locus of crustal magma differentiation and assimilation, driven by crustal thickening contemporaneous with increased tectonic convergence and ingression of the aseismic Juan Fernandez ridge, can account for all investigated aspects of the multi-Myr magmatic evolution leading up to the formation of the Rio Blanco-Los Bronces porphyry Cu deposits. Our findings corroborate the importance of high-pressure differentiation of hydrous magma for the formation of Andean-style porphyry deposits. Once magmas favourable for porphyry Cu mineralisation were generated in the lower crust, multiple episodes of efficient magma migration into the upper crust fed several, discrete, shallow magmatic-hydrothermal systems over ~3.5 Myr to form the world's largest known Cu resource at Rio Blanco-Los Bronces.

Key words: porphyry; copper; batholith; geochronology; petrogenesis

INTRODUCTION

Subduction results in a multitude of geological processes that impact humanity (e.g. earthquakes, volcanic eruptions, mineral resources). Arc magmas are particularly important agents of mass transfer into and through the crust, carrying volatiles and metals which may result in magmatic-hydrothermal mineralisation or be released through passive degassing or active eruptions. The chemical characteristics of arc magmas are the combined result of material fluxes from subducted crust that leads to melting of the overlying mantle wedge and subsequent fluid and melt transfer into the crust, where magmas differentiate and potentially assimilate crustal material (e.g. Elliott *et al.*, 1997; Turner *et al.*, 2017; Chiaradia *et al.*, 2020). Currently, views regarding the processes that exert the dominant control on arc magma chemistry vary significantly, with different models invoking varying components of partial melting of varying mantle source compositions, crustal melting, fractional crystallisation (FC) and crustal assimilation (DePaolo, 1981; Hildreth & Moorbath, 1988; Annen *et al.*, 2006; Clemens *et al.*, 2020). Identifying the contributions from the processes and sources controlling the chemistry of arc magmas is key to understanding the forces driving their petrogenesis and, ultimately, mineralisation.

The multitude of processes that could help to generate the array of arc magma compositions observed in nature is likely to vary significantly throughout the lifetime of a long-lived arc. Such arcs typically exhibit spatial and temporal variations in the dominant type of magmatic activity, including high-volume volcanism interspersed with quiescent periods ('flare-ups' and 'lulls'; e.g. Ducea, 2001). These spatiotemporal variations in magmatism have been related to changes in the tectonic regime and crustal thickness of the arc, where strong compression can result from the subduction of aseismic ridges and plateaus which leads to volcanic quiescence and low volcanic–plutonic ratios in arc

Received: November 28, 2023. **Revised:** February 21, 2024

products (Kay & Mpodozis, 2002; van Hunen *et al.*, 2002; Hollings *et al.*, 2005; Rosenbaum & Mo, 2011). During such tectonic events, the overall locus of magma evolution in the crust is expected to deepen, which may profoundly influence the composition of magmas that reach the upper crust (Müntener & Ulmer, 2018; Loucks, 2021). These periods have been linked to the formation of economically important, porphyry Cu(-Mo, -Au) systems (Cooke *et al.*, 2005; Rosenbaum *et al.*, 2005; Sillitoe, 2010).

The Andean margin hosts numerous magmatic-hydrothermal porphyry Cu deposits that formed in several narrow arc segments and restricted time windows (e.g. Sillitoe, 2010; Mpodozis & Cornejo, 2012; Spencer *et al.*, 2015; Buret *et al.*, 2016; Cernuschi *et al.*, 2018), typically towards the end of episodes of protracted magmatism (≥5–10 Myr; e.g. Bissig *et al.*, 2003; Chiaradia, 2009; Nathwani *et al.*, 2021). These deposits are commonly associated with volumetrically minor porphyry intrusions, which represent the uppermost expressions of vertically extensive magmatic systems (Dilles, 1987). They are often characterised by a specific geochemical affinity (e.g. high Sr/Y and high La/Yb) which provides clues to the nature of their underlying magmatic plumbing systems and the favourable conditions generated therein (Richards, 2011; Chiaradia *et al.*, 2012; Loucks, 2014). Being able to delineate and temporally resolve the magmatic arc processes and tectonic framework involved in generating conditions conducive for porphyry-ore-formation would yield critical insights into the controls of ore deposit genesis.

Here, we apply whole-rock (WR) geochemistry, Hf isotope geochemistry and zircon U–Pb geochronology to elucidate the processes driving the local, ~13.5 Myr evolution of arc magmas that formed the San Francisco Batholith (SFB) and associated Rio Blanco-Los Bronces porphyry deposit cluster, central Chile. Distinct temporal evolution in several geochemical indices (e.g. Sr/Y, La/Yb, Ba/Th, Th/La) during this period, combined with petrogenetic Monte Carlo (MC) modelling, provide important new insights into the origin and tempo of changes in the geodynamic environment and arc magma chemistry that play a key role in forming the world's largest porphyry Cu deposit cluster.

REGIONAL GEOLOGY

The SFB and the Rio Blanco-Los Bronces deposit cluster are located in the western Principal Cordillera of the central Chilean Andes. They are part of a north–south trending belt of late Miocene to early Pliocene porphyry Cu-deposit clusters (Fig. 1b). The Rio Blanco-Los Bronces porphyry cluster forms a ~10 km long, north-northwest-striking trend with a number of spatially and geologically separated deposits, each with their own hydrothermal systems, alteration stages, brecciation events and ore-associated porphyry intrusions (Fig. 1; e.g. Toro *et al.*, 2012). The combined mineralised centres make the Rio Blanco-Los Bronces district the world's largest known concentration of Cu with an original Cu resource of >200 Mt (Toro *et al.*, 2012). Here, we investigate the district along a southeast to northwest transect, taking in the Los Sulfatos deposit, the La Augustina deposit, the currently mined Los Bronces and Rio Blanco deposits, the San Manuel deposit and the older host rocks of the SFB (Fig. 1b). We will from here on refer to the intrusive rock suite of the SFB and the Rio Blanco-Los Bronces deposit clusters as the Rio Blanco-Los Bronces district.

The geodynamic setting of the Rio Blanco-Los Bronces district is unusual, sitting as it does in the transition between the Chilean Southern Volcanic Zone (~34–48°S), dominated by a normal subduction angle and abundant active volcanism and the flat-slab subduction of central Chile which has produced a eastward widening of the orogenic system and a lack of recent volcanic activity (Fig. 1a; Kay & Mpodozis, 2002). The oblique subduction of the aseismic Juan Fernandez ridge has been inferred as the trigger for flat-slab subduction in this region (Kay & Mpodozis, 2001, 2002 van Hunen *et al.*, 2002; Rosenbaum & Mo, 2011).

The Rio Blanco-Los Bronces porphyry cluster and the SFB are hosted by the dominantly volcanic and volcanosedimentary lithologies of the Eocene to Early Miocene Abanico Formation and the Miocene Farellones Formation (Piquer *et al.*, 2015). The SFB crops out in the central part of the inverted Abanico basin and is the largest intrusive complex in central Chile (~600 km^2). Zircon U–Pb geochronology suggests that protracted emplacement of calc-alkaline magmas occurred between ~16.5 and 8 Ma (Deckart *et al.*, 2014; Piquer *et al.*, 2015) with K-Ar geochronology on amphibole and biotite (~20 Ma; Warnaars *et al.*, 1985) and an older emplacement age (zircon U–Pb; 21.76 ± 0.53) for the Rio Colorado pluton situated immediately north of the SFB (Piquer *et al.*, 2015) hinting at even earlier intrusive phases. Some small porphyritic to sub-porphyritic intrusions are associated with uneconomic pulses of hydrothermal alteration and Cu mineralisation (15–8 Ma; Toro *et al.*, 2012) including the Los Piches, Ortiga and El Plomo prospects (Fig. 1).

The youngest set of intrusions in the district are Late Miocene to early Pliocene, subvolcanic, dacitic–rhyolitic porphyries and diatremes (~7–4.5 Ma) that were emplaced into the volcanic sequence and the older equigranular intrusions. They are thought to have been derived from a deeper, unexposed magma reservoir at 5–7 km depth, based on low V_p/V_s ratios in seismic tomography (Piquer *et al.*, 2015). The porphyries are coeval and spatially associated with abundant hydrothermal breccias in the mine areas and have been genetically related to the economic Cu–Mo mineralisation (Warnaars *et al.*, 1985; Deckart *et al.*, 2014). The post-ore La Copa diatreme at the northern end of the deposit cluster cross-cuts economic mineralisation and is considered the last magmatic expression in the district before a distinct relocation of igneous activity to the currently active volcanoes, ~30 km to the east.

METHODOLOGY

Whole-rock geochemical analysis

Thirty-one samples were collected from logged sections of drillcore and field outcrops from the SFB, porphyry intrusions associated with sub-economic mineralisation at Ortiga, Los Piches, El Plomo and San Manuel and porphyry intrusions from Los Sulfatos, La Augustina and Los Bronces that are associated with the giant porphyry deposit cluster and the La Copa diatreme (Fig. 1b). A set of 26 of these samples was analysed for their WR geochemistry by X-ray fluorescence (XRF) and laser ablation-inductively coupled plasma-mass spectrometry (LA-ICP-MS) at the University of Leicester. Major and trace element data were obtained by XRF analysis using a PANalytical Axios Advanced XRF spectrometer, equipped with a 4Kw Rh-anode end window X-ray tube. Trace element data were obtained from fusion beads using a New Wave 213 nm laser system linked to an iCAP-Qc quadrupole ICP-MS (Supplementary Table SA1). Further details on the analytical methodology and reference materials can be found in the Supplementary text and tables.

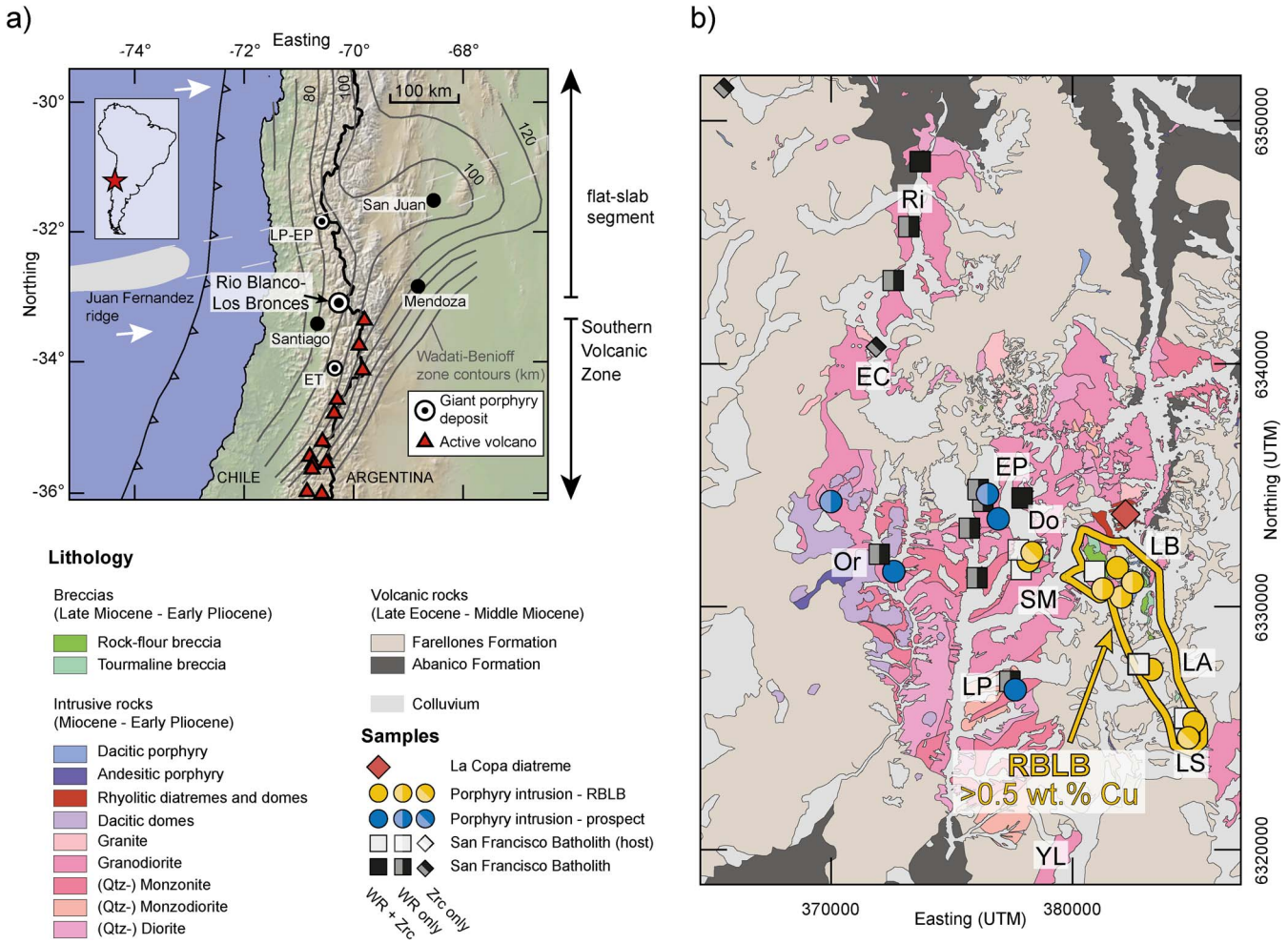

Fig. 1. Location and geological framework of the SFB and the Rio Blanco-Los Bronces (RBLB) porphyry deposit cluster (UTM zone 19H). (a) Regional topographic map of Central Chile and neighbouring Argentina (created with GeoMapApp) highlighting the three giant porphyry deposit clusters, Rio Blanco-Los Bronces, Los Pelambres-El Pachon (LP-EP) and El Teniente (ET). Contours of the Wadati-Benioff (from Anderson *et al.*, 2007; Perelló *et al.*, 2012) highlight contrasting slab angles north and south of the investigated area. Flat-slab subduction is related to the ingression of the Juan Fernandez ridge from the northwest. (b) District scale lithological map of the RBLB deposit cluster, SFB and surrounding volcanic lithologies (modified from Piquer *et al.*, 2015) including sample locations. Yellow contour highlights surface expression of domain-containing dominantly >0.5 wt.% Cu. This includes several spatially and temporally distinct deposits (Toro *et al.*, 2012). Do: Quebrada Dolores, EC: El Cruce, LA: La Agustina, LB: Los Bronces, LP: Los Piches, LS: Los Sulfatos, Or: Ortiga, Ri: Riecillos, SM: San Manuel, YL: Yerba Loca.

Zircon U–Pb geochronology and Hf isotope analysis

Zircons were extracted from 17 representative rocks for U–Pb geochronology and Hf isotope analysis. The rocks were crushed and zircons were separated with conventional techniques. All zircons were annealed for 48 hours at 900 °C, mounted in epoxy resin and polished to reveal their crystal interiors. Polished zircons were imaged using scanning electron microscope cathodoluminescence and back-scattered electron imaging using a Zeiss EVO SEM located in the Imaging and Analysis Centre (IAC), Natural History Museum (NHM), London. U–Pb isotopes in zircons were measured using an ESI-NWR 193 nm excimer laser coupled to an Agilent 7700x quadrupole ICP-MS, housed in the LODE Laboratory, IAC, NHM. The laser was operated with a 30-μm spot diameter, 5 Hz repetition rate and 2.5 J/cm^2 energy density. Analysis of the interior (core) and exterior (rim) or rim-only domains of individual zircon grains was conducted for every sample.

Adjacent spots were subsequently analysed for their ϵHf composition using a Thermo Fisher Scientific Neptune Plus MC-ICP-MS coupled to a New Wave Research 193FX Excimer laser ablation system at the Geochronology and Tracers Facility British Geological Survey, Keyworth, Nottingham. Helium was used as the carrier gas through the ablation cell with Ar make-up gas being connected via a T-piece and sourced from a Cetac Aridus II desolvating nebulizer. A low flow of nitrogen (8 ml/min) was introduced via the nebulizer, in addition to Ar, in order to minimise oxide formation. Lutetium (^{175}Lu), ytterbium (^{172}Yb, ^{173}Yb) and hafnium (^{176}Hf, ^{177}Hf, ^{178}Hf, ^{179}Hf and ^{180}Hf) isotopes were measured simultaneously during static 30-second ablation analyses. The spot size used was 25 μm at a repetition rate of 10 Hz and a fluence of ~9 J/cm^2. Details on the data reduction protocols are given in the Supplementary Material.

RESULTS

Zircon geochronology

Individual zircon ^{206}Pb/^{238}U dates from the 17 samples range from ~20 Ma to ~4 Ma (Fig. 2). Zircon data for each sample form an array in which individual dates dominantly overlap within individual 2σ uncertainty. A few analyses are resolvably older

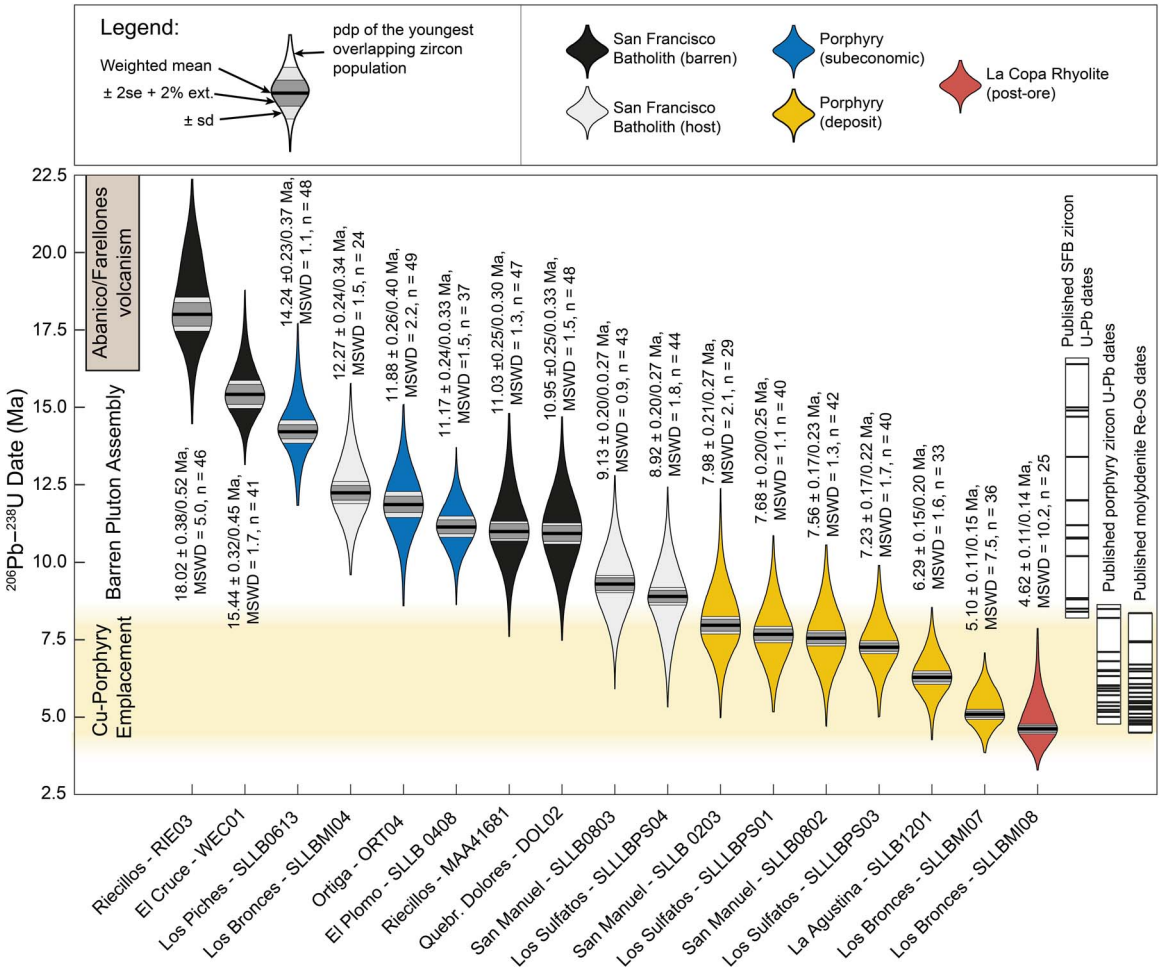

Fig. 2. Geochronology of the SFB and RBLB porphyry deposit cluster. Probability density plots (pdp) show the density of $^{206}Pb/^{238}U$ dates obtained for non-inherited zircons from each sample. Horizontal lines indicate the weighted mean for each sample. Dark grey boxes show the 2σ uncertainty for LA–ICP–MS $^{206}Pb/^{238}U$ dates including a propagated error of ±2%. Paler grey boxes illustrate standard deviation of all non-inherited zircons. Annotated dates are given with the two uncertainties, the MSWD and number of analyses. Samples are plotted left-to-right from oldest to youngest. Vertical line plots show literature zircon U–Pb dates for the SFB and RBLB porphyries (Toro *et al.*, 2012; Deckart *et al.*, 2014) and molybdenite Re-Os dates (Toro *et al.*, 2012).

(~10% of analyses) and these are considered to be inherited grains, or parts of grains. Such inheritance can be grouped into three main temporal windows: Miocene/Oligocene, Mesozoic and, rarely, Paleozoic (Supplementary Table SB6). Weighted mean dates were calculated for the overlapping, non-inherited zircon dates in each sample (Table 1). Weighted means of overlapping zircon dates are considered to represent a reasonable approximation of the magma emplacement age for each sample. The weighted means are assigned with the standard error (2se) including a 2% propagated uncertainty to account for excess variance and long-term, intra-lab reproducibility (cf. Horstwood *et al.*, 2016; Nathwani *et al.*, 2021). Additionally, the standard deviation (sd) and probability functions of the zircons from each sample are presented to illustrate the distributions in zircon dates and uncertainties, and the negligible impact they have on our age interpretations that are used to interpret the long-term (~16 Myr) magmatic evolution of the sample suite (Large *et al.*, 2020).

Mean-squared weighted deviations (MSWDs) range between <1 and 2.2 for most samples but are elevated for the oldest and youngest two samples (Table 1). The dispersion is attributed to either an actual spread of zircon crystallisation ages, unresolvable inheritance of xeno- and/or antecrysts (likely for the La Copa diatreme; SLLBMI08), the presence of unresolvable common Pb or Pb-loss or the underestimation of individual uncertainties. The weighted mean calculations that are ubiquitous in *in situ* geochronology are a measure to quantify the mean of a population while emphasising the importance of values with low uncertainties over those with high uncertainties and is valid in cases where the data are normally distributed around one expected value or over a range that is less than single data point precision (Wendt & Carl, 1991). However, zircons from individual samples crystallise over protracted timescales (Schoene *et al.*, 2012; Wotzlaw *et al.*, 2013; Samperton *et al.*, 2015). This is a feature of magmatic systems, but we consider our associated uncertainties (2se) including a 2% propagated uncertainty and sd appropriate for constraining an accurate emplacement age (Large *et al.*, 2020), particularly given that none of the conclusions of this work rely on 100 kyr precisions of the presented weighted means.

All analysed equigranular intrusive rocks of the SFB exhibit emplacement ages older than 8.5 Ma. Similar emplacement ages were obtained for the sub-economic porphyry occurrences distal to the Rio Blanco-Los Bronces porphyry cluster at Los Piches (14.24 ± 0.23/0.48 Ma), Ortiga (11.88 ± 0.26/0.6 Ma) and El Plomo (11.17 ± 0.24/0.34 Ma). Emplacement ages <8.5 Ma were exclusively obtained for porphyry intrusions within the Rio Blanco-Los Bronces deposit cluster and the La Copa diatreme.

Table 1: Summary of zircon LA-ICP-MS $^{206}Pb/^{238}U$ geochronology data from this study

Sample name	Deposit/region	Lithology	Weighted mean (Ma)	2se	2se + 2%	MSWD	n
RIE03	Riecillo	SFB	18.02	0.38	0.98	5.0	46
WEC01	W El Cruce	SFB	15.44	0.32	0.43	1.7	41
SLLB0613	Los Piches	Porphyry	14.24	0.23	0.48	1.1	48
SLLBMI04	Los Bronces Mine	SFB	12.27	0.24	0.51	1.5	24
ORT04	Ortiga	Porphyry	11.88	0.26	0.6	2.2	49
SLLB 0408	Plomo	Porphyry	11.17	0.24	0.34	1.5	37
MAA41681	Riecillo	SFB	11.03	0.25	0.6	1.3	47
DOL02	Quebrada Dolores	SFB	10.95	0.25	0.60	1.5	48
SLLB0803	San Manuel	SFB	9.31	0.20	0.47	0.9	43
SLLLBPS04	Los Sulfatos	SFB	8.92	0.20	0.56	1.8	44
SLLB0203	San Manuel	Porphyry	7.98	0.21	0.65	2.1	29
SLLLBPS01	Los Sulfatos	Porphyry	7.68	0.20	0.47	1.1	40
SLLB0802	San Manuel	Late Porphyry	7.56	0.17	0.51	1.3	42
SLLBPS03	Los Sulfatos	Late Porphyry	7.23	0.17	0.46	1.7	40
SLLB1201	La Augustina	Porphyry	6.29	0.15	0.34	1.6	33
SLLBMI07	Los Bronces Mine	Porphyry	5.10	0.11	0.45	7.5	36
SLLBMI08	Los Bronces Mine	La Copa Diatreme	4.62	0.11	0.68	10.2	25

The 2se refers to two times the standard error on the weighted mean calculation, and +2% refers to the propagation of an additional 2% external uncertainty. The MSWD refers to the mean squared weighted deviation, and *n* refers to the number of dates used to calculate the weighted mean date.

The oldest, overlapping, emplacement ages of porphyry intrusions within the cluster are from San Manuel and Los Sulfatos (7.98 ± 0.21/0.65, 7.23 ± 0.17/0.46 Ma). Emplacement ages of the La Agustina porphyry (6.29 ± 0.15/0.34 Ma) and the Don Luis porphyry (5.10 ± 0.11/0.45 Ma) at Los Bronces are resolvably younger. The emplacement of the post-ore La Copa diatreme (4.62 ± 0.11/0.68 Ma) is the last recorded event, in accordance with cross-cutting relationships.

Whole-rock geochemistry and zircon Hf isotopes

The WR data from the investigated samples were filtered by excluding samples with loss on ignition (LOI) >2 wt.% and those that clearly indicate hydrothermal alteration based on geochemical alteration indicators (Supplementary Figs S1 and S2). The investigated rock suite displays a large compositional variability (gabbroic to granitic) based on major element oxides, with no systematic difference between porphyritic and equigranular rocks (Fig. 3a–d). Concentrations of MgO (<7 wt.%), TiO_2 (<1.2 wt.%) and Al_2O_3 (<20 wt.%) decrease systematically with increasing SiO_2 (50–74 wt.%; Fig. 3b–d). However, trace element contents differ markedly between the pre-8.5 Ma rocks (i.e. the equigranular rocks of the SFB and early porphyritic intrusions) and the younger porphyritic intrusions associated with the giant Cu deposits (Fig. 3d–i). The pre 8.5 Ma rocks illustrate sub-horizontal or shallow downward trends of La/Yb and Sr/Y with increasing SiO_2, whereas the younger porphyry intrusions display elevated values for these trace element ratios (Fig. 3d–i).

Combining the geochronology data with geochemical WR information reveals that major element compositional indicators, such as SiO_2, MgO and TiO_2 (Fig. 4a–c), scatter unsystematically over time from 18 Ma until the emplacement of the La Copa diatreme (~4.5 Ma). However, systematic, unidirectional and continuous shifts are apparent for several trace element ratios (e.g. increasing Sr/Y, Ba/Th, Dy/Yb, V/Sc and Eu/Eu* and decreasing Th/La; Fig. 4b–i). Values of ϵHf plotted against the single spot date for the same zircon domain highlight a decrease in ϵHf over time (Fig. 5a). Even when considering the associated uncertainties, it is possible to resolve a trend of slightly decreasing ϵHf (by about 2 units) over 9 Myr from ~18 Ma to ~9 Ma, which is followed by a more rapid decrease by ~2 ϵHf units in the following 4 Myr until the emplacement of the La Copa diatreme. WR Ba/Th and Th/La correlate with average ϵHf in non-inherited zircons from the same samples (Fig. 5b).

DISCUSSION

Protracted pluton assembly culminating in episodic formation of giant ore deposits

The derived emplacement ages for the SFB and subsequent porphyries span a range of ~13.5 Myr (18.02 ± 0.38/0.52 Ma to 4.62 ± 0.11/0.14 Ma), illustrating the protracted assembly of the intrusive complex. The oldest intrusive pulse recorded in this study occurred ~5 Myr earlier than suggested by previous U–Pb zircon geochronology (Fig. 2; Toro *et al.*, 2012; Deckart *et al.*, 2014), but is consistent with K-Ar hornblende and biotite data (Warnaars *et al.*, 1985). The onset of batholith assembly broadly coincides with a waning of prior, widespread volcanic activity at ~16 Ma as represented by the outcropping Abanico and Farellones Formations (Fig. 2; Hollings *et al.*, 2005; Piquer *et al.*, 2015). This transition from dominantly volcanic to intrusive magmatism can be reconciled with the general geodynamic framework in Central Chile, where increased convergence since the late Oligocene (Pardo-Casas & Molnar, 1987) led to a continuously more compressive environment and crustal thickening from ~22 Ma (Kay & Mpodozis, 2002; Riesner *et al.*, 2019). A more compressional stress regime could have hindered magma migration through the crust, limiting effusive volcanism (Kay & Mpodozis, 2002; Rosenbaum *et al.*, 2005). Instead, magmas stalled in the mid to upper crust, leading to assembly of the large Miocene plutonic complexes in Central Chile. Similar transitions from volcanism

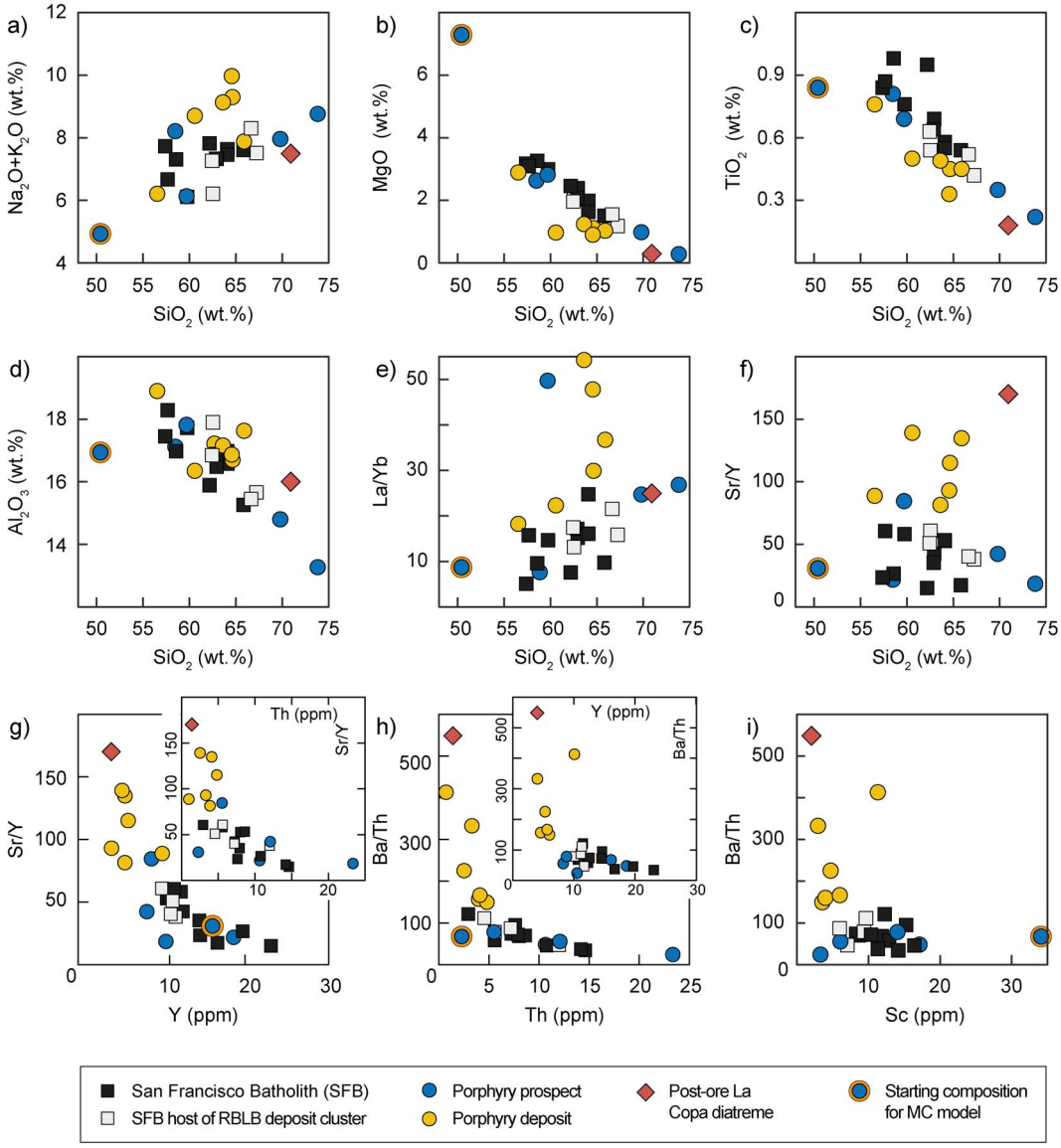

Fig. 3. Covariation diagrams of all bulk-rock geochemical data from least-altered rocks obtained in this study. Major elements resolve geochemical variation between samples (a–d). Trace element contents differ between older equigranular rocks of the SFB and porphyry prospects and younger porphyry intrusions of the San Manuel deposit and the RBLB deposit cluster (d–i), with systematic trends evident for Ba/Th and Sr/Y as a function of Th, Y and Sc (g–i). Small inset plots in (g) and (h) highlight correlation between Sr/Y and Th as well as Ba/Th and Y. Blue circle with orange shade is the least evolved sample of the dataset and was used as the starting composition for the modelling.

to pluton assembly have been recorded in other major porphyry districts (e.g. Arizona: Lang & Titley, 1998; Yerington, Nevada: Dilles & Wright, 1988, Quellaveco, Peru: Nathwani *et al.*, 2021).

The early, voluminous (>90% of exposed intrusive rocks) but subeconomic period of growth of the intermediate to felsic SFB (18–9 Ma; Fig. 2) overlaps with the emplacement of other Miocene plutons of Central Chile (e.g. La Gloria, Yerba Loca, Mesón Alto, Portillo; Deckart *et al.*, 2010). This temporal overlap with plutonic magmatism in the Central Chilean Principal Cordillera more generally (~32°S–35°S) indicates that mid- to upper-crustal intrusive magmatism occurred along an arc-parallel axis over >100 km in the mid-Miocene. This oldest SFB age (Riecillo; 18.02 ± 0.38/0.52 Ma) is found in the north west of the SFB and is located proximal to the older Rio Colorado pluton (21.76 ± 0.53 Ma) and may suggest a progressive younging of emplacement ages to the south east of the complex. In contrast, few intrusions have been identified that were emplaced contemporaneously with the mineralised Late Miocene to Pliocene porphyry intrusions in the Rio Blanco-Los Bronces district (~8 to ~4.5 Ma; Fig. 2), with El Teniente (~6.3 to ~4.4 Ma) being a notable example of temporal overlap (Maksaev *et al.*, 2004; Spencer *et al.*, 2015). This could be the result of an exposure-related bias (e.g. erosion of shallowly emplaced porphyries), but the spatial concentration of intrusive activity related to the mineralised centres at Rio Blanco-Los Bronces and El Teniente suggests that these systems are products of highly focused magmatism, perhaps during a shift to transient transpressional periods within a progressively more compressional environment (Piquer *et al.*, 2021).

The overlap between the ages of syn- and post-ore porphyry intrusions in the Rio Blanco-Los Bronces district with published molybdenite Re-Os dates (~8–5 Ma; Fig. 2; Toro *et al.*, 2012; Deckart *et al.*, 2014) strongly supports the inference that these porphyries are the shallow crustal igneous expression of the evolving

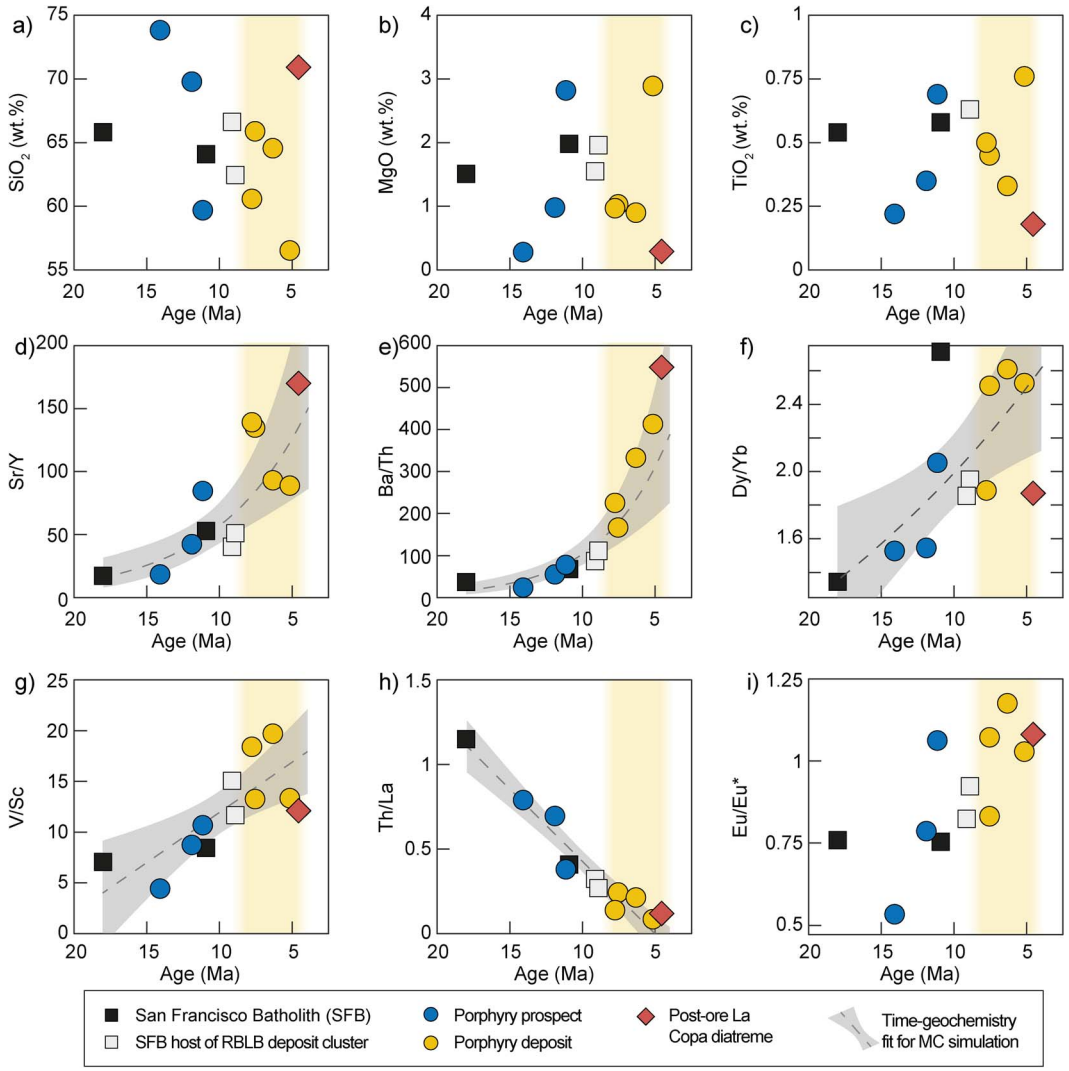

Fig. 4. Temporally resolved variations in magma chemistry displayed by plotting weighted mean dates against bulk-rock data. Major components such as SiO_2 vary unsystematically over time (a–c), whereas trace elements (d–i) display a clear temporal progression to higher Sr/Y, Ba/Th, Dy/Yb, V/Sc, Eu/Eu∗ and lower Th/La values over time. Dotted lines are statistical fits through the time-geochemistry plots with the pale grey field highlighting the uncertainty envelope. These fits are used to filter MC simulations for valid runs for individual time increments. Analytical uncertainty is smaller than the symbol size in all cases.

magmatic-hydrothermal system that formed the Cu deposits (Dilles, 1987; Sillitoe, 2010), despite the observation that alteration–mineralisation overprints them. The porphyry intrusions at San Manuel and Los Sulfatos overlap within uncertainty and field relationships indicate that the main ore-forming event in each of these systems ended before emplacement of the post-ore porphyries in these two centres (7.56 ± 0.17/0.51 Ma—SLLB0802 and 7.23 ± 0.17/0.46—SLLBPS03). Although the temporal resolution of the presented LA-ICP-MS U–Pb data are insufficient to accurately and precisely constrain the duration of the ore-forming events, the data are in accordance with short timescales as inferred from chemical abrasion-isotope dilution-thermal ionisation mass spectrometry (CA-ID-TIMS) geochronology, hydrothermal modelling and diffusion timescale studies in other porphyry systems (<200 kyr and potentially as little as a few 10 s of kyr: Weis *et al.*, 2012; Buret *et al.*, 2016; Cernuschi *et al.*, 2018; Large *et al.*, 2020). Based on the emplacement ages of syn-mineralisation porphyry intrusions at La Augustina (6.29 ± 0.15/0.34 Ma—SLLB1201) and Los Bronces (5.10 ± 0.11/0.45 Ma—SLLBMI07), the main ore-forming events in these deposits occurred resolvably after ore formation at San Manuel and Los Sulfatos. Thus, we propose that the construction of the giant Cu resource at Rio Blanco-Los Bronces resulted from several, temporally and spatially discrete, magmatic-hydrothermal events.

Multi-Myr evolution in arc magma chemistry and potential controls

The major element data highlight compositional diversity but plot along the same calc-alkaline fractionation trends of increasing $Na_2O + K_2O$ and decreasing MgO, TiO_2 and Al_2O_3 with increasing SiO_2 (Fig. 3a–c), consistent with liquid lines of descent established by experiments (Müntener & Ulmer, 2018; Ulmer *et al.*, 2018). However, these trends represent magma evolution over ~13.5 Myr (Fig. 4a–c) and do not represent a single differentiation path through time. The convoluted major element patterns over time (Fig. 4a–c) contrast with observations from many porphyry districts where there is a general temporal trend towards more evolved compositions (Bissig *et al.*, 2003; Chiaradia, 2009; Nathwani *et al.*, 2021). However, systematic temporal trends in trace elements are observed in the Rio Blanco-Los Bronces

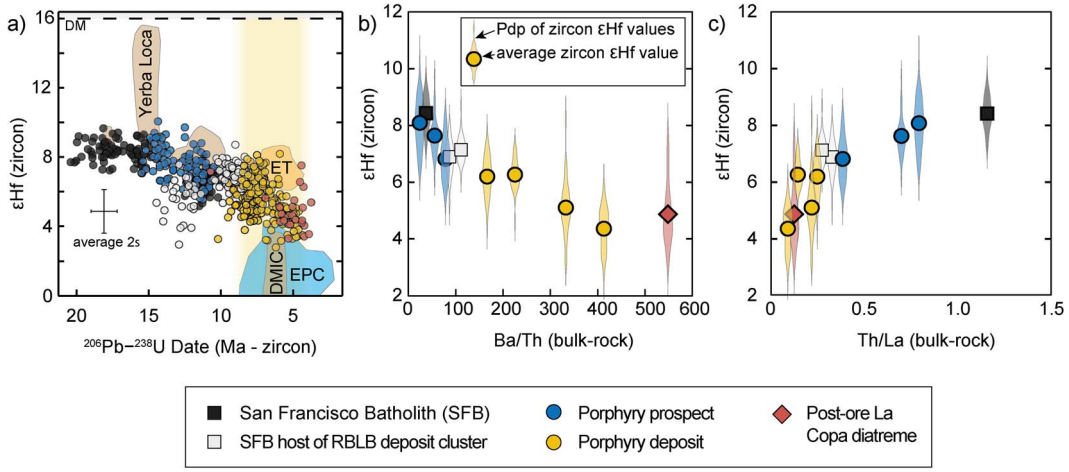

Fig. 5. Zircon ϵHf and bulk-rock Ba/Th and Th/La systematics of the investigated rock suite. (a) Individual zircon dates plotted against ϵHf value of the same zircon domain. Yellow band represents the period of economic mineralisation. Area above the dotted line represents DM values. Shaded fields represent literature data (Muñoz *et al.*, 2013; Gilmer *et al.*, 2018 and references therein) for Central Chile; blue—Eastern Principal Cordillera (EPC), dark orange—Don Manuel intrusive complex (DMIC), orange—El Teniente (ET), brown—equigranular intrusions of Central Chile (including the Yerba Loca pluton). (b) Range (probability density plots) and average (circles) of ϵHf values for each sample correlate with Ba/Th and Th/La ratios of the corresponding bulk-rock sample.

district (Fig. 4), indicating decoupling between these and the major components, akin to the variable compositions over time observed in the El Abra porphyry Cu district, Northern Chile (Rabbia *et al.*, 2017) and the Meghri-Ordubad pluton, Lesser Caucasus (Rezeau *et al.*, 2017). This is best explained by trace element contents recording differences in the source melt composition or in the crustal magmatic plumbing system (e.g. differences in the assimilation fractional crystallisation (AFC) and/or rejuvenation systematics) with only a minor contribution to their signatures by the degree of melt differentiation (Hildreth & Moorbath, 1988; Annen *et al.*, 2006).

Elevated ratios of light rare-earth elements (LREE) and mid rare-earth elements (MREE) over heavy rare-earth elements (HREE) (high La/Yb and Dy/Yb) as well as high Sr/Y and V/Sc in the ore-related porphyry intrusions (Figs 3 and 4) are in agreement with observations from other porphyry deposits (Bissig *et al.*, 2003; Chiaradia *et al.*, 2009; Loucks, 2014; Nathwani *et al.*, 2021), but such features can also be observed in hydrous arc-related, calc-alkaline igneous rocks unrelated to porphyry deposits (e.g. Profeta *et al.*, 2016), especially those formed in thickened crust (e.g. Northern Southern Volcanic Zone: Hickey-Vargas *et al.*, 2016; Turner *et al.*, 2017). These signatures have been associated with lower-plate processes, such as subduction erosion (Kay & Mpodozis, 2002) or an inhomogeneous mantle source (Turner *et al.*, 2017), but are in most cases attributed to crustal processes, such as partial melting of the lower crust (Bissig *et al.*, 2003; Munoz *et al.*, 2012; Qian & Hermann, 2013) or the fractional crystallisation of different mineral assemblages (Rohrlach & Loucks, 2005; Chiaradia *et al.*, 2012; Nathwani *et al.*, 2021). The ratio of plagioclase to amphibole (± clinopyroxene, garnet) in the crystallising assemblage, which is controlled by the depth of crystallisation and the water content of the crystallising melt, is expected to play a key role in the evolution of these trace element systematics (Alonso Perez *et al.*,, 2008; Richards, 2011; Chiaradia *et al.*, 2012).

Barium and Th have typically not been interpreted when investigating the geochemistry of porphyry ore-forming magmas due to their unsystematic behaviour but, at Rio Blanco-Los Bronces, we record well-defined trends of increasing Ba/Th and decreasing Th/La over time, mainly driven by decreasing Th contents in the WR samples (Fig. 3h). In subduction-related magmas with limited crustal melt modification, Th/La is considered to be coupled to the composition of the subducted sediments (Plank, 2005), whereas Ba/Th can yield insights into the fluid or melt component derived from the lower-plate (Pearce *et al.*, 2005). However, thick crust in the investigated arc segment (Kay & Mpodozis, 2002; Riesner *et al.*, 2019) and the differentiated nature of the emplaced magmas (Fig. 3) mean that crustal processes are likely to have overprinted original mantle signatures. Crustal controls on Ba and Th systematics by deep crustal, hot zone assimilation and partial melting of host rocks with variable Ba/Th have been recently suggested (Qian & Hermann, 2013; Chiaradia *et al.*, 2020).

Based on current intra-crustal fractionation models for the derivation of porphyry wholerock signatures (Richards, 2011; Loucks, 2014; Chiaradia & Caricchi, 2017), the correlation between such ratios (Sr/Y, La/Yb, Dy/Yb, V/Sc, etc) and Ba/Th or Th/La (Fig. 3g and h) supports the inference that the latter signatures result largely from the same set of intra-crustal processes, or that an interplay of sub- and intra-crustal processes are driving their evolution. The ratios Ba/Th and Th/La further correlate with Hf isotope and Sc systematics of zircons from the same samples (Figs 3i, 5b,c). Decreasing Sc is considered to mainly result from the fractionation of amphibole and/or clinopyroxene (e.g. Lee *et al.*, 2005) that are abundant in most crustal crystallisation assemblages (DeBari & Greene, 2011; Müntener & Ulmer, 2018), whereas low ϵHf can be a robust tracer of crustal melting and assimilation (e.g. Gilmer *et al.*, 2018; Storck *et al.*, 2020). Because high Ba/Th ratios correlate with low Sc values (high degrees of crustal differentiation) and lower zircon ϵHf (higher degree of assimilation and/or assimilation of a more radiogenic component), we conclude that crustal contributions are increasingly significant in the younger magmas of the Rio Blanco-Los Bronces district. Henceforward, we explore how crustal FC and AFC processes may have controlled the evolution of the arc magma signatures identified.

Testing intra-crustal drivers for trace element evolution in arc magmas in thickening crust using a Monte Carlo approach

We use petrogenetic modelling following a Monte Carlo approach to test whether crustal processes can account for the clear time-geochemistry trajectories identified at Rio Blanco-Los

Bronces. Two end-member models were run, considering FC and AFC processes. The modelling approach allows assessment of the relative importance of changes in the crystallisation assemblage and assimilant in producing the observed trace element evolution. Identification of different crystallisation assemblages can provide constraints on the petrogenetic conditions during magma evolution (e.g. depth and water content), whereas constraints on the assimilant composition can provide insight into the crustal lithologies involved and their potential host terrane.

Model set-up and results

In each modelled scenario, we ran 1 500 000 simulations in which the melt composition was calculated at every 2.5% crystallisation increment to a crystallinity of 80% (i.e. F = 0.2). Elements considered were Ba, Th, Sr, Y, V, Sc, La, Dy and Yb. The fractionating crystal assemblage consisted of variable proportions of the minerals expected during mid- to lower-crustal fractionation of arc magmas (plagioclase, amphibole, clinopyroxene, orthopyroxene, apatite, magnetite, rutile ± garnet; DeBari & Greene, 2011; Müntener & Ulmer, 2018; Ulmer *et al.*, 2018). The assemblage was varied for each simulation but, for simplicity, was kept constant during crystallisation in each simulation (see Supplementary Tables SA2 and SA3 for details on the modelling conditions). We additionally tested each scenario with and without garnet in the crystallising assemblage because of the recent debate on whether garnet is present in the fractionating mineral assemblage of porphyry-related magmas (e.g. Lee & Tang, 2020; Tatnell *et al.*, 2023). Partition coefficients were selected for each simulation from a range of published data (See Supplementary Table SA3) to allow the model to account for the complexities in modelling trace element ratios (e.g. Tatnell *et al.*, 2023) related to selected partition coefficients. In the FC and AFC scenarios, we used a constant initial melt composition based on the most mafic intrusion analysed in this study (50 wt.% SiO_2), which is a basaltic porphyry dike at El Plomo that intruded the SFB (SLLB0412, see Fig. 3). The composition of assimilated material was randomly varied within a reasonable range based on potential basement lithologies as identified by previous work in the Frontal Cordillera and Coastal Cordillera (Supplementary Table SA2). The mass ratio of assimilated material to crystallised material varied between 0 (no assimilation) and 0.6 (e.g. Chiaradia *et al.*, 2020).

No pure FC simulations can fully account for the geochemical diversity of rocks from the Rio Blanco-Los Bronces district (Fig. 6). FC can reproduce the variability in Sr/Y (Fig. 6a) confirming a strong control of the crystallising assemblage on the bulk-magma partition coefficients of this ratio (Loucks, 2014; Chiaradia & Caricchi, 2017; Nathwani *et al.*, 2021). However, it fails to produce sufficient variation in Ba/Th, Th and Th/La (Fig. 6c and e), as none of the crystallising minerals efficiently fractionate Ba or Th from the melt (Supplementary Table SA3). The AFC model, on the other hand, can reproduce the geochemical variability of the natural data (Fig. 6b, d, f), both for Sr-Y and Ba-Th-La systematics, suggesting that the involvement of crustal assimilation is required to account for the geochemical evolution identified in the Rio Blanco-Los Bronces district over ~13.5 Myr. The AFC models are hereafter further explored for information they can provide on the petrogenetic controls resulting in the observed time-chemistry trends.

Petrogenetic implications of the AFC Monte Carlo modelling results

Using the MC model outcomes, we have attempted to identify the dominant drivers for the evolution of different trace element

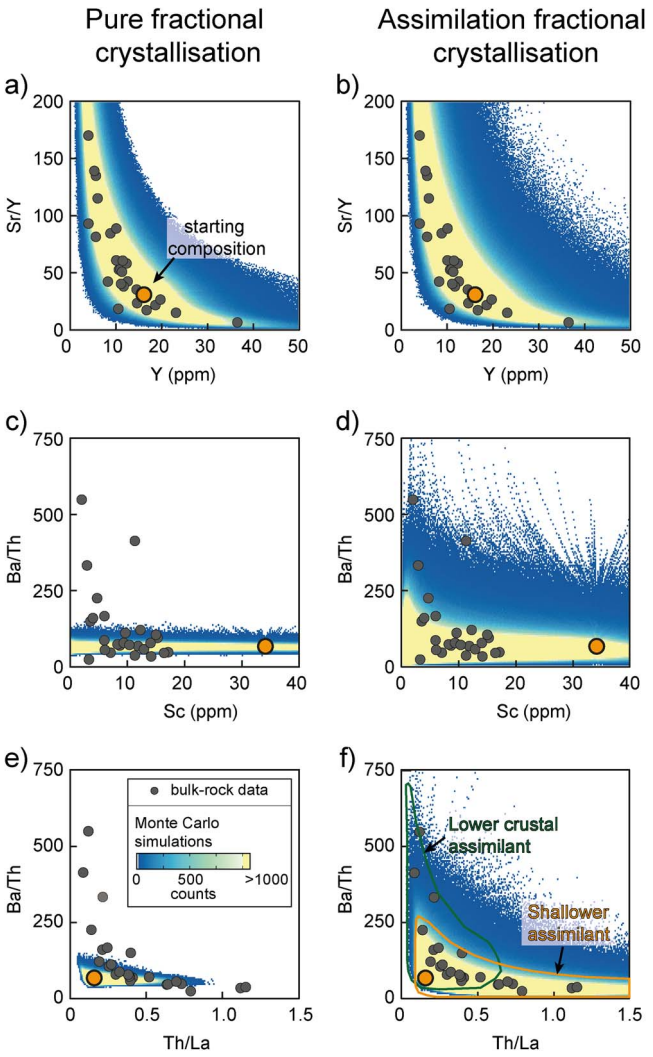

Fig. 6. Density maps of all results of the two end-member MC simulation approaches, pure FC and AFC. The FC model records the effect on the melt geochemistry of different crystallising assemblages from a common starting composition. The AFC model further considers assimilation of material that ranges in composition based on the different potential crustal lithologies in Central Chile (see Supplementary Material for a detailed list). Grey points indicate bulk-rock composition of natural rock samples and orange points highlight the starting composition; this was fixed based on the most primitive sample identified in the study (50 wt.% SiO_2: also indicated in Fig. 3). Variations in Sr/Y, Y and Sc recorded in the natural rock suite are reproduced by both models. Natural variation in Ba/Th versus Th/La cannot be accounted for by the pure FC model but can be accounted for by varying amounts of the different assimilants. Green and orange outlines in (f) highlight the >500 MC model count areas using the suggested deeper (Kay *et al.*, 1996) and shallower crustal assimilant compositions (Llambías *et al.*, 2003), respectively.

systematics. Regressions through the time-geochemistry plots from the Rio Blanco-Los Bronces district (Fig. 4c–f and Supplementary Material 1) were used to filter the Monte Carlo data for parameter combinations that can account for the observed temporal trends. A parameter set is only considered valid if a fractionation step can account for all geochemical criteria in the models (Ba/Th, Sr/Y, Th/La, V/Sc, Dy/Yb, Th) within any 0.5 Ma time interval between 18 and 5 Ma.

The AFC modelling suggests that the temporal evolution trends of Sr/Y, V/Sc and Dy/Yb observed in the Rio Blanco-Los Bronces district do not require a specific change in assimilant composition.

The trends can be derived from nearly the entire range of potential assimilant compositions because the model predicts a broad range and stable median of the assimilant compositon over time (see medians and violin plots in Fig. 7c, d). Furthermore, as indicated by the pure fractional crystallisation model, the evolution of these ratios can be simply explained by a temporal evolution of the fractionating assemblage, with an initial dominance of plagioclase (>50%; Fig. 7a, b) and progressive modal increase of amphibole ± pyroxene (at the expense of plagioclase), which ultimately become the dominant fractionating phases at ~9 Ma (Fig. 7a, b). This shift can be explained by magma fractionation at higher pressures (above about 7 kbar) and/or at higher H_2O_{melt} (above about 6 wt.%; e.g. Alonso-Perez *et al.*, 2008; Chiaradia *et al.*, 2012).

Models run with garnet as a fractionating mineral phase indicate that garnet is not required to generate Rio Blanco-Los Bronces magma compositions (Fig. 7) and <0.5% garnet was present as a fractionating phase in the simulations that best reproduce the whole rock trends. Thus, we conclude that garnet fractionation is not required to account for porphyry Cu whole rock signatures in general (e.g. high Sr/Y and La/Yb), in accordance with other modelling work (Tatnell *et al.*, 2023), and is therefore unlikely to play a significant role in arc magma oxidation and porphyry Cu deposit formation (Holycross & Cottrell, 2023). Nonetheless, garnet crystallisation will occur in the deepest crustal levels of thickened crust (>0.8 GPa; Alonso-Perez *et al.*, 2008) but derivative HREE-depleted melt compositions could be readily overprinted by subsequent amphibole fractionation at shallower crustal levels (Davidson *et al.*, 2007) so that the garnet signature of such geodynamic settings may be challenging to fingerprint.

The inferred transition towards strongly amphibole-fractionated magma compositions over time in the Rio Blanco-Los Bronces district provides insights into the tectonomagmatic evolution of the area. The behaviour can be accounted for by magma differentiation at a higher pressure and/or at higher H_2O_{melt}, both of which will be promoted by a strongly compressive tectonic regime (van Hunen *et al.*, 2002; Chiaradia *et al.*, 2020). In Central Chile, this can be attributed to the progressively more compressional tectonic regime during the Miocene that has been linked to increased tectonic convergence, ingression of the Juan Fernandez ridge and consequent slab-flattening (Kay & Mpodozis, 2002). This change in geodynamics could have promoted 'auto-hydration' by extended lower-crustal fractionation (Rohrlach & Loucks, 2005; Chiaradia & Caricchi, 2017; Loucks, 2021).

The observed trends in Ba/Th and Th/La (Fig. 4) and concentrations of Th require a significant change in assimilant composition at around 9 Ma as constrained by 'successful' MC model outputs (Fig. 7e, f). To account for the recorded geochemical trends in the district the average assimilant must have evolved from high Th, low Ba compositions to low Th, high Ba in tandem with the change in the dominant crystallising assemblage (Figs 6 and 7). It has been proposed that the Principal Cordillera is underlain by the basement of the Chilenia block and the underlying and older Cuyania terrane (Ramos, 2010), with both considered to correspond to Proterozoic Laurentian crust formed in an island-arc setting (Kay *et al.*, 1996). The Choyoi Formation, and other outcropping lithologies of the Chilenia terrane (See Supplementary Material), have low Ba/Th ratios (median = 78) and could therefore have been the main assimilant during the early stage of magma evolution, at the inferred shallower crustal depths (Figs 7e, f and 8). Rare evidence of potential lower-crustal assimilants from the Cuyania terrane exhibit high Ba/Th (median = 1200). Thus, the increase

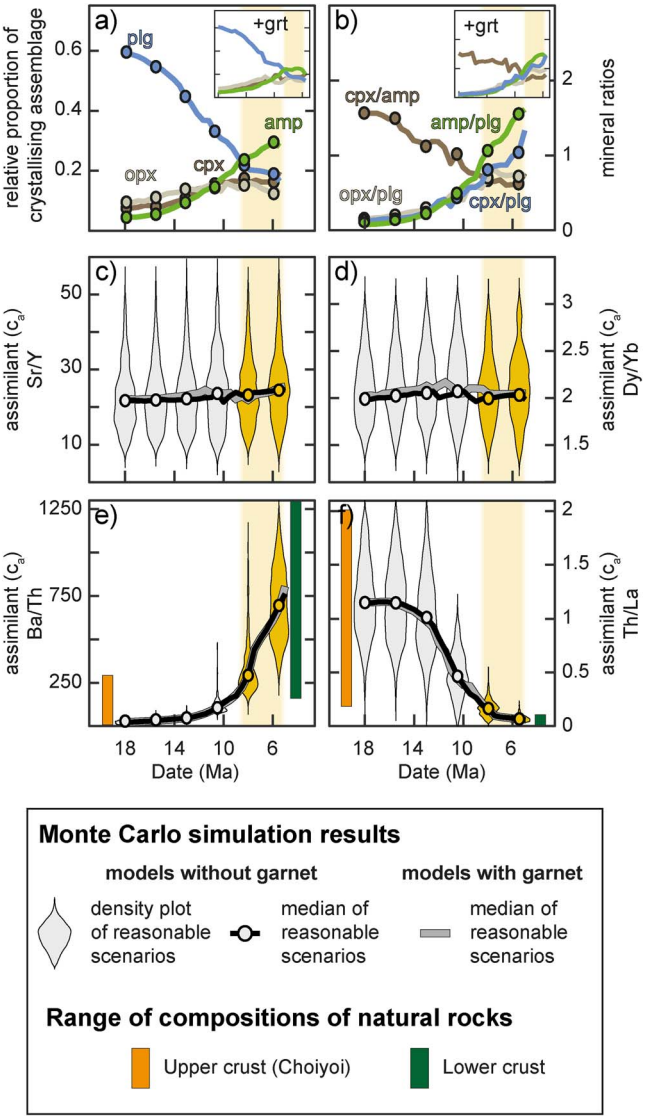

Fig. 7. Magmatic evolution of the investigated arc segment based on the AFC MC petrogenetic modelling approach. Lines highlight median values of conditions extracted from simulations that reproduce the observed whole rock geochemical trends over time (Fig. 4 and Supplementary Material 1). Lines connect 0.5 Ma time increments (18–4.5 Ma). Violin plots illustrate variability in boundary conditions for successful simulations at 18, 15.5, 13, 10.5, 8 and 5.5 Ma. (a) and (b) illustrate the variation in the required crystallising assemblage. Inset shows that simulations are near identical when garnet is included as a fractionating phase (garnet is not included amongst the other minerals on this plot since it is present in vanishingly small proportions in the mode ouputs (<0.005; Supplementary Fig. S7)). (c)–(f) record the required assimilant composition to account for successful modelling runs with grey lines showing comparable results when garnet is included. Modelled assimilant compositions covered nearly the entire range of the x-axis in (c)–(f). Orange and green boxes in (e) and (f) illustrate ranges in compositions of the Choiyoi Formation, a potential shallower-crustal assimilant (Llambías *et al.*, 2003) and lower-crustal xenoliths, an alternative deep crustal assimilant (Kay *et al.*, 1996), respectively.

in Ba/Th and decrease in Th/La of emplaced magmas with time could be related to a progressively deeper locus of hot-zone AFC processes involving increasing assimilation of Cuyania terrane rocks, consistent with the inferred higher pressure environment of FC (Figs 7e, f and 8). Increased magma interaction with the Cuyania terrane rocks may be related to the presence of an eastward verging thrust fault between the two

terranes causing the Chilenia block to progressively override the Cuyania block during compression and crustal thickening (Fig. 8; Muñoz *et al.*, 2013).

The important role of a shift in the locus of magma evolution in the generation of the geochemical signatures of the magmas in the Rio Blanco-Los Bronces district is in accordance with the Hf isotope trajectory of zircons (Fig. 5). The trend towards less radiogenic Hf signatures with time (Fig. 5a) mirrors the spatial shift to less radiogenic Hf (and Nd) isotopic signatures recorded in whole rock data from the Western to the Eastern Principal Cordillera (Muñoz *et al.*, 2013). This transition has been attributed to a shift from dominantly Chilenia block assimilation in the west to a greater influence from the underlying Cuyania terrane in the east (see Fig. 8).

The temporal geochemical evolution observed in this study displays similar characteristics to spatial variability in geochemistry noted in other Andean settings, such as the Ecuadorian arc (Chiaradia *et al.*, 2020). Here, the spatial geochemical variability along the arc is proposed to have resulted from subduction of the aseismic Carnegie ridge that led to a deeper average locus of arc magma evolution in the arc segment immediately above the ridge (Chiaradia *et al.*, 2020). Our preferred geodynamic interpretation for the SFB and the Rio Blanco-Los Bronces district follows along similar lines except for the oblique nature of the ridge subduction in Central Chile which resulted in a southward migration of peak compression with time leading to the pronounced temporal variability in one location.

Potential contributions of lower plate processes on the observed geochemical evolution

In this study, we test a model for the Central Chilean Miocene to Pliocene arc evolution in which the geochemical signatures of the magmas are solely controlled by crustal processes, thus ignoring potential variation of the composition of source magmas derived from the lower plate and mantle wedge. In subduction magmas with limited crustal melt modification, Th/La and Ba/Th are considered to be influenced by subducted sediments and the depth and degree of devolatilisation and melting of the mantle (Pearce *et al.*, 2005; Plank, 2005). There is no evidence for a change in the type of subducted sediments in the Miocene of Central Chile (Hildreth & Moorbath, 1988) that could explain the observed geochemical trends, tending to rule out this possibility. However, shallowing of the slab and an associated decrease in the depth of fluid/melt derivation could help to explain temporal increases in Ba/Th and decreases in Th/La. Early, steep subduction would have favoured the release of components such as Ba, Th ± Nb, that can be extracted from the slab at greater depths (Elliott *et al.*, 1997). Later derivation of greater fluid volumes (in which Ba is more mobile) from the shallowing slab could have promoted the generation of higher Ba/Th magmas entering the crust (Pearce *et al.*, 2005). However, because all rocks investigated in this study crystallised from evolved magmas, the systematic change in geochemical signatures would need to be retained during extended differentiation and development of the other geochemical signatures (e.g. Sr/Y, Dy/Yb) that are more readily explained by crustal processes. This lower plate scenario would also struggle to account for the systematically decreasing ϵHf signatures over time, which are coupled with the aforementioned trace element ratios. Hafnium-isotopic signatures from the nearby Yerba Loca pluton (5 km south-east of the SFB) range from depleted mantle (DM)-like compositions to more radiogenic compositions at ~16 Ma, also pointing to a DM-like source that

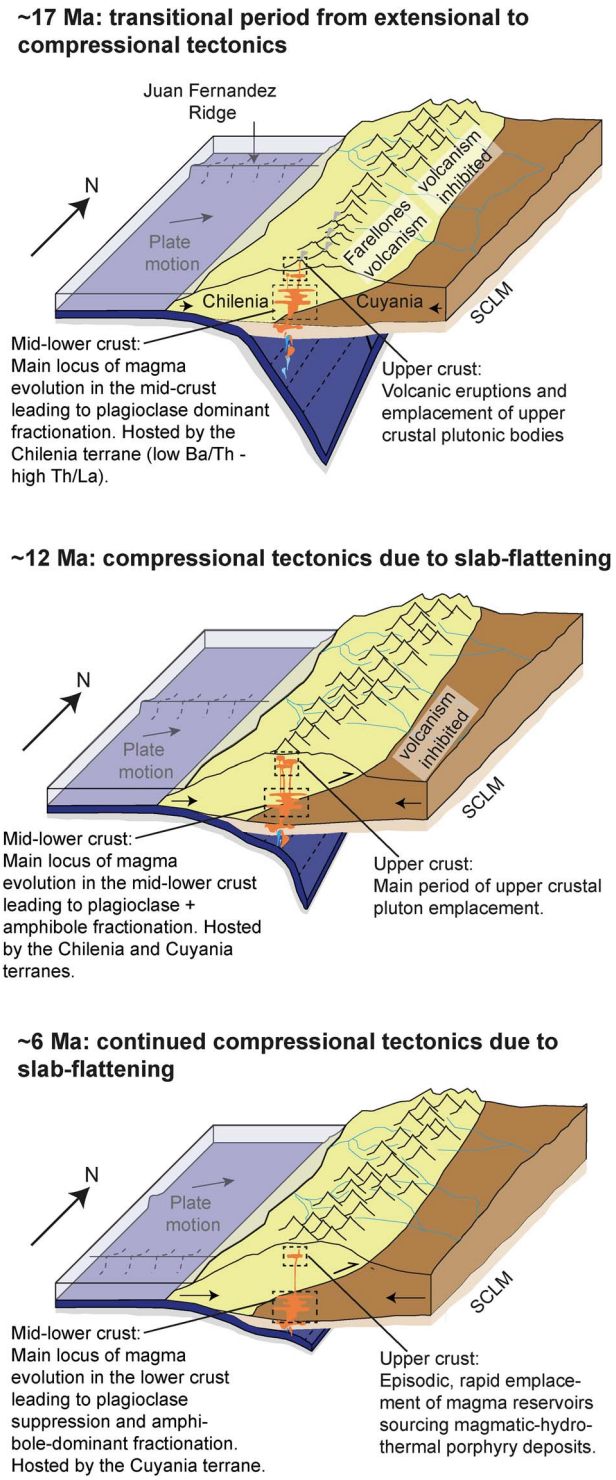

Fig. 8. Schematic illustration of the Miocene tectono-magmatic evolution suggested for the Central Chilean arc segment. Cross-section is at the latitude of the Rio Blanco-Los Bronces district. Gradual ingression of the Juan Fernandez ridge leads to increased compression, flatter slab subduction, crustal thickening, cessation of volcanic activity and a progressively deeper locus of main magma evolution. Increased compression caused progressive overriding of the Chileania terrane over the Cuyania terrane along an active east-vergent reverse fault (Farías *et al.*, 2010). The giant ore deposits were formed in multiple episodes over 3.5 Myr, linked to magmas that were efficiently extracted from the lower crust into shallower domains during transient transpressional periods within a progressively more compressional environment.

progressively equilibrated with crustal lithologies (Deckart *et al.*, 2010). Thus, although we cannot exclude a lower plate influence on the evolution of magmas in the Rio Blanco-Los Bronces district, we conclude that such a control is not required to account for the changes leading up to porphyry Cu deposit formation at Rio Blanco-Los Bronces.

Implications for the genesis of porphyry Cu deposits in magmatic arcs

Uneconomic porphyry prospects were formed throughout the assembly of the SFB (>13.5 Myr; Fig. 1) but the Rio Blanco-Los Bronces porphyry deposit cluster, Earth's largest identified economic accumulation of Cu, formed in the final 3.5 Myr following batholith construction. The clear transition in the tectonic and crustal framework of magmatism is proposed to have driven deeper and more hydrous magma evolution, which has been suggested as a key step in the formation of economic Andean-style porphyry deposits (Bissig *et al.*, 2003; Hollings *et al.*, 2005; Chiaradia *et al.*, 2009; Munoz *et al.*, 2012; Chelle-Michou *et al.*, 2015; Loucks, 2021; Nathwani *et al.*, 2021). Several non-mutually exclusive reasons have been proposed for the association of arc magmas fractionated at high pressures with economic porphyry deposit formation. These include high magmatic H_2O contents which enhance fluid and metal extraction (Richards, 2011; Chiaradia & Caricchi, 2017; Rezeau & Jagoutz, 2020), high oxidation state which may enhance sulphur and metal solubility (Lee & Tang, 2020) and also that deep crustal reservoirs provide optimal conditions for the acccumulations of large magma volumes that can deliver larger amounts of metal and fluid to the upper crust (Chelle-Michou & Rottier, 2021; Chiaradia, 2022).

A notable aspect of our study is the duration of assembly of the precursor SFB over ca. 9 Myr. An extended period of barren pluton assembly followed by giant porphyry Cu deposit formation is observed in other porphyry Cu districts, including the Fortuna Complex (Chuquicamata, Northern Chile; Campbell *et al.*, 2006), the Yarabamba Batholith (Quellaveco, Toquepala and Cuajone, Southern Peru; Simmons *et al.*, 2013; Nathwani *et al.*, 2021) and the Meghri-Ordubad pluton (Kadjaran, southern Armenia; Rezeau *et al.*, 2016). However, this relationship is not typical of smaller systems. Large-scale precursor pluton assembly may represent a key step in the formation of the largest porphyry Cu systems because extended magmatism would lead to heating and viscous behaviour of the crust, potentially favouring the accumulation of large magma volumes and inhibiting volcanic venting and loss of volatiles (Chelle-Michou & Rottier, 2021). Prolonged storage of fluid-saturated magmas at mid-upper crustal depths for >100 kyr durations (Karakas *et al.*, 2017; Large *et al.*, 2021) has been identified as a critical stage in the formation of porphyry copper deposits (Large *et al.* 2021, Nathwani *et al.*, 2023).

Previous studies of arc magma evolution in porphyry Cu districts have suggested both a progressive transition of trace element compositions over Myr durations (Rohrlach & Loucks, 2005; Nathwani *et al.*, 2021) or a more abrupt shift over 100 kyr durations (Hollings *et al.*, 2005; Chiaradia *et al.*, 2009; Carter *et al.*, 2022). The geochemical record preceding economic Cu ore-formation at Rio Blanco-Los Bronces (>10 My) appears to be of the former type, apparently exhibiting a gradational change in bulk-rock chemistry. However, we note that the nature of the sample suite and the geochronological precision imply that, in this study, it is not possible to delineate sudden transient geochemical excursions (beyond the 10^6 yr resolution) from and within the long-term, rather unidirectional trend.

The focusing of hydrous magma emplacement into the small sector at Rio Blanco-Los Bronces after ~8.5 Ma is thought to have been mediated by a few key structures during transient transpression (Piquer *et al.*, 2021). This control could have promoted rapid magma migration into the upper crust (Chiaradia & Caricchi, 2017; Large *et al.*, 2021) without requiring a significant change in the bulk magma flux. The focused extraction of magmas from deeper levels into the upper crust could have accreted sufficiently sized magma reservoirs to source the major porphyry deposits. After venting of the late and barren La Copa rhyolite, magmatism terminated in the district and migrated ~20–40 km to the southeast, potentially as a result of an excessively compressive environment and re-adjustment of the tectono-magmatic architecture (e.g. Gianni & Luján, 2021).

The similarly sized Cu resources (Toro *et al.*, 2012) of the early Los Sulfatos deposit (~7.5 Ma; Fig. 2) compared to the younger Los Bronces deposit (~5.5 Ma; Fig. 2) indicate that the potential to form a giant ore deposit did not change between 8 and 5 Ma. Thus, we propose that once magma compositions favourable for (giant) ore-formation were established (~10–8 Ma), other processes, such as the flux of hydrous magma, the thermal state of the crust, the efficiency of magma transport and focused exsolution of metal-charged fluids were the controlling factors on when, where and to what extent ore deposition occurred. Whereas most individual porphyry Cu deposits suggest short durations of ore-formation (<200 kyr) 'super-giant' porphyry clusters, such as the Central Chilean Rio Blanco-Los Bronces, Los Pelambres-El Pachon and El Teniente systems record porphyry emplacement and molybdenite Re-Os dates that spread over several Myr (Maksaev *et al.*, 2004; Cannell *et al.*, 2005; Spencer *et al.*, 2015). This suggests that relatively long-lived, focused magmatism and superposition of several, likely discrete, upper-crustal magmatic-hydrothermal systems is a requirement for generating the largest copper accumulations (e.g. Chelle-Michou *et al.*, 2017; Chiaradia & Caricchi, 2017).

CONCLUSIONS

We present a comprehensive WR, geochronological and zircon ϵHf dataset from the SFB and the Rio Blanco-Los Bronces district that allows investigation of changes in arc magmatism within a ~25 km arc segment over ~13.5 My. Monte Carlo simulations suggest systematic temporal changes in crustal fractionation and assimilation acted as the main drivers of trace element trends. Based on the strong correlations between trace element ratios and Hf isotope systematics, we suggest that the geochemical evolution can be explained by a progressive deepening of the main locus of magma differentiation coupled with substantive assimilation of progressively deeper, Proterozoic crustal domains. These changes are consistent with increased tectonic convergence and the progressive ingression of the Juan Fernandez ridge from the north-west, promoting a compressional tectonic environment, flat slab subduction, inhibition of volcanism and consequent deepening of the primary crustal magma reservoir that progressively fed the growth of the mid-upper crustal SFB. From ~10–8 Ma onwards, deep crustal processes generated magma compositions that were favourable for economic porphyry Cu deposit formation. The subsequent, relatively stable arc architecture then allowed multiple episodes of upward magma migration to be structurally focused into the Rio Blanco-Los Bronces district. This led to the establishment and partial superimposition of several discrete porphyry ore-forming magmatic-hydrothermal systems over ~3.5 Myr to produce the world's largest known concentration of Cu.

ACKNOWLEDGEMENTS

This study was funded by the NERC Highlight Topic award 'FAMOS' (From arc magmas to ores) via NE/P017452/1 (NHM), NE/P017053/1 (Leicester) and NE/P01724X/1 (British Geological Survey). We thank Tiffany Barry for assistance with the laser ablation WR trace element data acquisition and Callum Hatch for sample preparation. Field sampling and logistical support from Anglo American and the Anglo Chile team, in particular Sebastien Ramirez, Ricardo Boric, Pablo Villegas and the technical staff, is greatly appreciated. Massimo Chiaradia, Jose Piquer and Bob Loucks are thanked for their constructive reviews of this manuscript. We thank all members of the FAMOS research consortium for many insightful discussions during the course of this research.

DATA AVAILABILITY

The data underlying this article are available in the article and in its online supplementary material. The R Code used for the petrogenetic modelling is archived at: https://doi.org/10.5281/zenodo.10210941

SUPPLEMENTARY DATA

Supplementary data are available at *Journal of Petrology* online.

References

Alonso-Perez, R., Müntener, O. & Ulmer, P. (2008). Igneous garnet and amphibole fractionation in the roots of island arcs: experimental constraints on andesitic liquids. *Contributions to Mineralogy and Petrology* **157**, 541–558.

Anderson, M., Alvarado, P., Zandt, G. & Beck, S. (2007). Geometry and brittle deformation of the subducting Nazca plate, Central Chile and Argentina. *Geophysical Journal International* **171**, 419–434. https://doi.org/10.1111/j.1365-246X.2007.03483.x.

Annen, C., Blundy, J. D. & Sparks, R. S. J. (2006). The genesis of intermediate and silicic magmas in deep crustal hot zones. *Journal of Petrology* **47**, 505–539. https://doi.org/10.1093/petrology/egi084.

Bissig, T., Clark, A. H., Lee, J. K. W. & von Quadt, A. (2003). Petrogenetic and metallogenetic responses to Miocene slab flattening: new constraints from the El Indio-Pascua Au–Ag–Cu belt, Chile/Argentina. *Mineralium Deposita* **38**, 844–862. https://doi.org/10.1007/s00126-003-0375-y.

Buret, Y., von Quadt, A., Heinrich, C., Selby, D., Wälle, M. & Peytcheva, I. (2016). From a long-lived upper-crustal magma chamber to rapid porphyry copper emplacement: Reading the geochemistry of zircon crystals at Bajo de la Alumbrera (NW Argentina). *Earth and Planetary Science Letters* **450**, 120–131. https://doi.org/10.1016/j.epsl.2016.06.017.

Cannell, J., Cooke, D. R., Walshe, J. L. & Stein, J. (2005). Geology, mineralization, alteration, and structural evolution of the El Teniente porphyry Cu-Mo deposit. *Economic Geology* **100**, 979–1003. https://doi.org/10.2113/gsecongeo.100.5.979.

Campbell, I. H., Ballard, J. R., Palin, J. M., Allen, C. & Faunes, A. (2006). U-Pb zircon geochronology of granitic rocks from the Chuquicamata-El Abra porphyry copper belt of northern Chile: excimer laser ablation ICP-MS analysis. *Economic Geology* **101**, 1327–1344. https://doi.org/10.2113/gsecongeo.101.7.1327.

Carter, L. C., Tapster, S. R., Williamson, B. J., Buret, Y., Selby, D., Rollinson, G. K., Millar, I. & Parvaz, D. B. (2022). A rapid change in magma plumbing taps porphyry copper deposit-forming magmas. *Scientific Reports* **12**, 17272. https://doi.org/10.1038/s41598-022-20158-y.

Cernuschi, F., Dilles, J. H., Grocke, S. B., Valley, J. W., Kitajima, K. & Tepley, F. J. (2018). Rapid formation of porphyry copper deposits evidenced by diffusion of oxygen and titanium in quartz. *Geology* **46**, 611–614. https://doi.org/10.1130/G40262.1.

Chelle-Michou, C. & Rottier, B. (2021). Transcrustal magmatic controls on the size of porphyry Cu systems–State of knowledge and open questions. *Society of Economic Geologists Special Publication, No. 24, Vol. 1. Tectonomagmatic Influences on Metallogeny and Hydrothermal Ore Deposits: A Tribute to Jeremy P. Richards*. https://doi.org/10.5382/SP.24.06.

Chelle-Michou, C., Chiaradia, M., Béguelin, P. & Ulianov, A. (2015). Petrological evolution of the magmatic suite associated with the Coroccohuayco Cu(−Au–Fe) porphyry–skarn deposit, Peru. *Journal of Petrology* **56**, 1829–1862. https://doi.org/10.1093/petrology/egv056.

Chelle-Michou, C., Rottier, B., Caricchi, L. & Simpson, G. (2017). Tempo of magma degassing and the genesis of porphyry copper deposits. *Scientific Reports* **7**, 40566. https://doi.org/10.1038/srep40566.

Chiaradia, M. (2009). Adakite-like magmas from fractional crystallization and melting-assimilation of mafic lower crust (Eocene Macuchi arc, Western cordillera, Ecuador). *Chemical Geology* **265**, 468–487. https://doi.org/10.1016/j.chemgeo.2009.05.014.

Chiaradia, M. (2022). Distinct magma evolution processes control the formation of porphyry cu–au deposits in thin and thick arcs. *Earth and Planetary Science Letters* **599**, 117864. https://doi.org/10.1016/j.epsl.2022.117864.

Chiaradia, M. & Caricchi, L. (2017). Stochastic modelling of deep magmatic controls on porphyry copper deposit endowment. *Scientific Reports* **7**, 44523. https://doi.org/10.1038/srep44523.

Chiaradia, M., Merino, D. & Spikings, R. (2009). Rapid transition to long-lived deep crustal magmatic maturation and the formation of giant porphyry-related mineralization (Yanacocha, Peru). *Earth and Planetary Science Letters* **288**, 505–515. https://doi.org/10.1016/j.epsl.2009.10.012.

Chiaradia, M., Ulianov, A., Kouzmanov, K. & Beate, B. (2012). Why large porphyry cu deposits like high Sr/Y magmas? *Scientific Reports* **2**, 685. https://doi.org/10.1038/srep00685.

Chiaradia, M., Müntener, O. & Beate, B. (2020). Effects of aseismic ridge subduction on the geochemistry of frontal arc magmas. *Earth and Planetary Science Letters* **531**, 115984. https://doi.org/10.1016/j.epsl.2019.115984.

Clemens, J. D., Stevens, G. & Bryan, S. E. (2020). Conditions during the formation of granitic magmas by crustal melting – hot or cold; drenched, damp or dry? *Earth Science Reviews* **200**, 102982. https://doi.org/10.1016/j.earscirev.2019.102982.

Cooke, D. R., Hollings, P. & Walshe, J. L. (2005). Giant porphyry deposits: characteristics, distribution, and tectonic controls. *Economic Geology* **100**, 801–818. https://doi.org/10.2113/gsecongeo.100.5.801.

Davidson, J., Turner, S., Handley, H., Macpherson, C. & Dosseto, A. (2007). Amphibole "sponge" in arc crust? *Geology* **35**, 787. https://doi.org/10.1130/G23637A.1.

DeBari, S. M. & Greene, A. R. (2011). Vertical stratification of composition, density, and inferred magmatic processes in exposed arc crustal sections. *Arc-Continent Collision*. Springer, 121–144. https://doi.org/10.1007/978-3-540-88558-0_5.

Deckart, K., Godoy, E., Bertens, A., Jerez, D. & Saeed, A. (2010). Barren Miocene granitoids in the central Andean metallogenic belt, Chile: geochemistry and Nd-Hf and U-Pb isotope

systematics. *Andean. Geology* **37**, 1–31. https://doi.org/10.4067/S0718-71062010000100001.

Deckart, K., Silva, W., Spröhnle, C. & Vela, I. (2014). Timing and duration of hydrothermal activity at the Los Bronces porphyry cluster: an update. *Mineralium Deposita* **49**, 535–546. https://doi.org/10.1007/s00126-014-0512-9.

DePaolo, D. J. (1981). Trace element and isotopic effects of combined wallrock assimilation and fractional crystallization. *Earth and Planetary Science Letters* **53**, 189–202. https://doi.org/10.1016/0012-821X(81)90153-9.

Dilles, J. H. (1987). Petrology of the Yerington batholith, Nevada; evidence for evolution of porphyry copper ore fluids. *Economic Geology* **82**, 1750–1789. https://doi.org/10.2113/gsecongeo.82.7.1750.

Dilles, J. H. & Wright, J. E. (1988). The chronology of early Mesozoic arc magmatism in the Yerington district of western Nevada and its regional implications. *GSA Bulletin* **100**, 644–652. https://doi.org/10.1130/0016-7606(1988)100<0644:TCOEMA>2.3.CO;2.

Ducea, M. (2001). The California arc: thick granitic batholiths, eclogitic residues, lithospheric-scale thrusting, and magmatic flare-ups. *GSA Today* **11**, 4–10. https://doi.org/10.1130/1052-5173(2001)011<0004:TCATGB>2.0.CO;2.

Elliott, T., Plank, T., Zindler, A., White, W. & Bourdon, B. (1997). Element transport from slab to volcanic front at the Mariana arc. *Journal of Geophysical Research: Solid Earth* **102**, 14991–15019. https://doi.org/10.1029/97JB00788.

Farías, M., Comte, D., Charrier, R., Martinod, J., David, C., Tassara, A., Tapia, F. & Fock, A. (2010). Crustal-scale structural architecture in Central Chile based on seismicity and surface geology: implications for Andean mountain building. *Tectonics* **29**. https://doi.org/10.1029/2009TC002480.

Gianni, G. M. & Luján, S. P. (2021). Geodynamic controls on magmatic arc migration and quiescence. *Earth Science Reviews* **218**, 103676. https://doi.org/10.1016/j.earscirev.2021.103676.

Gilmer, A. K., Sparks, R. S. J., Blundy, J. D., Rust, A. C., Hauff, F., Hoernle, K., Spencer, C. J. & Tapster, S. (2018). Petrogenesis and assembly of the Don Manuel igneous complex, miocene–pliocene porphyry copper belt, Central Chile. *Journal of Petrology* **59**, 1067–1108. https://doi.org/10.1093/petrology/egy055.

Hickey-Vargas, R., Holbik, S., Tormey, D., Frey, F. A. & Moreno Roa, H. (2016). Basaltic rocks from the Andean southern volcanic zone: insights from the comparison of along-strike and small-scale geochemical variations and their sources. *Lithos* **258-259**, 115–132. https://doi.org/10.1016/j.lithos.2016.04.014.

Hildreth, W. & Moorbath, S. (1988). Crustal contributions to arc magmatism in the Andes of Central Chile. *Contributions to Mineralogy and Petrology* **98**, 455–489. https://doi.org/10.1007/BF00372365.

Hollings, P., Cooke, D. & Clark, A. (2005). Regional geochemistry of tertiary igneous rocks in Central Chile: implications for the geodynamic environment of giant porphyry copper and epithermal gold mineralization. *Economic Geology* **100**, 887–904. https://doi.org/10.2113/gsecongeo.100.5.887.

Holycross, M. & Cottrell, E. (2023). Garnet crystallization does not drive oxidation at arcs. *American Association for the Advancement of Science* **380**, 506–509. https://doi.org/10.1126/science.ade3418.

Horstwood, M. S. A., Košler, J., Gehrels, G., Jackson, S. E., McLean, N. M., Paton, C., Pearson, N. J., Sircombe, K., Sylvester, P., Vermeesch, P., Bowring, J. F., Condon, D. J. & Schoene, B. (2016). Community-derived standards for LA-ICP-MS U-(Th-)Pb geochronology – uncertainty propagation, age interpretation and data reporting. *Geostandards and Geoanalytical Research* **40**, 311–332. https://doi.org/10.1111/j.1751-908X.2016.00379.x.

van Hunen, J., Van Den, B. E. R. G. & A. P. & Vlaar, N. J. (2002). On the role of subducting oceanic plateaus in the development of shallow flat subduction. *Tectonophysics* **352**, 317–333. https://doi.org/10.1016/S0040-1951(02)00263-9.

Karakas, O., Degruyter, W., Bachmann, O. & Dufek, J. (2017). Lifetime and size of shallow magma bodies controlled by crustal-scale magmatism. *Nature Geoscience* **10**, 446–450. https://doi.org/10.1038/ngeo2959.

Kay, S. M. & Mpodozis, C. (2001) Central Andean ore deposits linked to evolving shallow subduction systems and thickening crust. *GSA Today* **11**, 4. https://doi.org/10.1130/1052-5173(2001)011<0004:CAODLT>2.0.CO;2.

Kay, S. M. & Mpodozis, C. (2002). Magmatism as a probe to the neogene shallowing of the Nazca plate beneath the modern Chilean flat-slab. *Journal of South American Earth Sciences* **15**, 39–57.

Kay, S. M., Orrell, S. & Abbruzzi, J. (1996). Zircon and whole rock Nd-Pb isotopic evidence for a Grenville age and a Laurentian origin for the basement of the Precordillera in Argentina. *The Journal of Geology* **104**, 637–648. https://doi.org/10.1086/629859.

Lang, J. R. & Titley, S. R. (1998). Isotopic and geochemical characteristics of Laramide magmatic systems in Arizona and implications for the genesis of porphyry copper deposits. *Economic Geology* **93**, 138–170. https://doi.org/10.2113/gsecongeo.93.2.138.

Large, S. J. E., Wotzlaw, J.-F., Guillong, M., von Quadt, A. & Heinrich, C. A. (2020). Resolving the timescales of magmatic and hydrothermal processes associated with porphyry deposit formation using zircon U–Pb petrochronology. *Geochronology* **2**, 209–230. https://doi.org/10.5194/gchron-2-209-2020.

Large, S. J. E., Buret, Y., Wotzlaw, J. F., Karakas, O., Guillong, M., von Quadt, A. & Heinrich, C. A. (2021). Copper-mineralised porphyries sample the evolution of a large-volume silicic magma reservoir from rapid assembly to solidification. *Earth and Planetary Science Letters* **563**, 116877. https://doi.org/10.1016/j.epsl.2021.116877.

Lee, C.-T. A. & Tang, M. (2020). How to make porphyry copper deposits. *Earth and Planetary Science Letters* **529**, 115868. https://doi.org/10.1016/j.epsl.2019.115868.

Lee, C.-T. A., Leeman, W. P., Canil, D. & Li, Z.-X. A. (2005). Similar V/Sc systematics in MORB and arc basalts: implications for the oxygen fugacities of their mantle source regions. *Journal of Petrology* **46**, 2313–2336. https://doi.org/10.1093/petrology/egi056.

Llambías, E. J., Quenardelle, S. & Montenegro, T. (2003). The Choiyoi group from Central Argentina: a subalkaline transitional to alkaline association in the craton adjacent to the active margin of the Gondwana continent. *Journal of South American Earth Sciences* **16**, 243–257. https://doi.org/10.1016/S0895-9811(03)00070-1.

Loucks, R. R. (2014). Distinctive composition of copper-ore-forming arcmagmas. *Australian Journal of Earth Sciences* **61**, 5–16. https://doi.org/10.1080/08120099.2013.865676.

Loucks, R. R. (2021). Deep entrapment of buoyant magmas by orogenic tectonic stress: its role in producing continental crust, adakites, and porphyry copper deposits. *Earth Science Reviews* **220**, 103744. https://doi.org/10.1016/j.earscirev.2021.103744.

Maksaev, V., Munizaga, F., McWilliams, M., Fanning, M., Mathur, R., Ruiz, J. & Zentilli, M. (2004). New chronology for El Teniente, Chilean Andes, from U-Pb, 40Ar/39Ar, Re-Os, and fission-track dating: Implications for the evolution of a supergiant porphyry Cu-Mo deposit. *Society of Economic Geologists* **11**, 15–54. https://doi.org/10.5382/SP.11.02.

Mpodozis, C. & Cornejo, P. (2012). Cenozoic Tectonics and Porphyry Copper Systems of the Chilean Andes. *Society of Economic Geologists Special Publication* **16**, *329–360, Geology and Genesis of Major*

Copper Deposits and Districts of the World A Tribute to Richard H. Sillitoe https://doi.org/10.5382/SP.16.14.

Munoz, M., Charrier, R., Fanning, C. M., Maksaev, V. & Deckart, K. (2012). Zircon trace element and O-Hf isotope analyses of mineralized intrusions from El Teniente ore deposit, Chilean Andes: constraints on the source and magmatic evolution of porphyry Cu-Mo related magmas. *Journal of Petrology* **53**, 1091–1122. https://doi.org/10.1093/petrology/egs010.

Muñoz, M., Farías, M., Charrier, R., Fanning, C. M., Polvé, M. & Deckart, K. (2013). Isotopic shifts in the Cenozoic Andean arc of Central Chile: records of an evolving basement throughout cordilleran arc mountain building. *Geology* **41**, 931–934. https://doi.org/10.1130/G34178.1.

Müntener, O. & Ulmer, P. (2018). Arc crust formation and differentiation constrained by experimental petrology. *American Journal of Science* **318**, 64–89. https://doi.org/10.2475/01.2018.04.

Nathwani, C. L. , Large, S. J. E., Brugge, E. R., Wilkinson, J. J., Buret, Y. & EIMF (2023). Apatite evidence for a fluid-saturated, crystalrich magma reservoir forming the Quellavecoporphyry copper deposit (Southern Peru). *Contributions to Mineralogy and Petrology* **178**, 49. https://doi.org/10.1007/s00410-023-02034-8.

Nathwani, C. L., Simmons, A. T., Large, S. J. E., Wilkinson, J. J., Buret, Y. & Ihlenfeld, C. (2021). From long-lived batholith construction to giant porphyry copper deposit formation: petrological and zircon chemical evolution of the Quellaveco District, southern Peru. *Contributions to Mineralogy and Petrology* **176**, 12. https://doi.org/10.1007/s00410-020-01766-1.

Pardo-Casas, F. & Molnar, P. (1987). Relative motion of the Nazca (Farallon) and south American plates since late cretaceous time. *Tectonics* **6**, 233–248. https://doi.org/10.1029/TC006i003p00233.

Pearce, J. A., Stern, R. J., Bloomer, S. H. & Fryer, P. (2005). Geochemical mapping of the Mariana arc-basin system: implications for the nature and distribution of subduction components. *Geochemistry, Geophysics, Geosystems* **6**. https://doi.org/10.1029/2004GC000895.

Perelló, J., Sillitoe, R., Mpodozis, C., Brockway, H. & Posso, H. (2012). Geologic setting and evolution of the porphyry copper-molybdenum and copper-gold deposits at Los Pelambres, Central Chile. *Society of Economic Geologists* , 79–104. https://doi.org/10.5382/SP.16.04.

Piquer, J., Skarmeta, J. & Cooke, D. R. (2015). Structural evolution of the Rio Blanco-Los Bronces District, Andes of Central Chile: controls on stratigraphy, magmatism, and mineralization. *Economic Geology* **110**, 1995–2023. https://doi.org/10.2113/econgeo.110.8.1995.

Piquer, J., Sanchez-Alfaro, P. & Pérez-Flores, P. (2021). A new model for the optimal structural context for giant porphyry copper deposit formation. *Geology* **49**, 597–601. https://doi.org/10.1130/G48287.1.

Plank, T. (2005). Constraints from thorium/lanthanum on sediment recycling at subduction zones and the evolution of the continents. *Journal of Petrology* **46**, 921–944. https://doi.org/10.1093/petrology/egi005.

Profeta, L., Ducea, M. N., Chapman, J. B., Paterson, S. R., Gonzales, S. M. H., Kirsch, M., Petrescu, L. & DeCelles, P. G. (2016). Quantifying crustal thickness over time in magmatic arcs. *Scientific Reports* **5**, 17786. https://doi.org/10.1038/srep17786.

Qian, Q. & Hermann, J. (2013). Partial melting of lower crust at 10–15 kbar: constraints on adakite and TTG formation. *Contributions to Mineralogy and Petrology* **165**, 1195–1224. https://doi.org/10.1007/s00410-013-0854-9.

Rabbia, O. M., Correa, K. J., Hernández, L. B. & Ulrich, T. (2017). "Normal" to adakite-like arc magmatism associated with the El Abra porphyry copper deposit, Central Andes, Northern Chile. *International Journal of Earth Sciences* **106**, 2687–2711. https://doi.org/10.1007/s00531-017-1454-0.

Ramos, V. A. (2010). The Grenville-age basement of the Andes. *Journal of South American Earth Sciences* **29**, 77–91. https://doi.org/10.1016/j.jsames.2009.09.004.

Rezeau, H. & Jagoutz, O. (2020). The importance of H2O in arc magmas for the formation of porphyry cu deposits. *Ore Geology Reviews* **126**, 103744. https://doi.org/10.1016/j.oregeorev.2020.103744.

Rezeau, H., Moritz, R., Wotzlaw, J.-F., Tayan, R., Melkonyan, R., Ulianov, A., Selby, D., d'Abzac, F.-X. & Stern, R. A. (2016). Temporal and genetic link between incremental pluton assembly and pulsed porphyry cu-Mo formation in accretionary orogens. *Geology* **44**, 627–630. https://doi.org/10.1130/G38088.1.

Rezeau, H., Moritz, R., Leuthold, J., Hovakimyan, S., Tayan, R. & Chiaradia, M. (2017). 30 Myr of Cenozoic magmatism along the Tethyan margin during Arabia–Eurasia accretionary orogenesis (Meghri–Ordubad pluton, southernmost lesser Caucasus). *Lithos* **288-289**, 108–124. https://doi.org/10.1016/j.lithos.2017.07.007.

Richards, J. P. (2011). High Sr/Y arc magmas and porphyry cu ± Mo ± au deposits: just add water. *Economic Geology* **106**, 1075–1081. https://doi.org/10.2113/econgeo.106.7.1075.

Riesner, M., Simoes, M., Carrizo, D. & Lacassin, R. (2019). Early exhumation of the frontal cordillera (southern Central Andes) and implications for Andean mountain-building at ~33.5 degrees S. *Scientific Reports* **9**, 7972. https://doi.org/10.1038/s41598-019-44320-1.

Rohrlach, B. D. & Loucks, R. R. (2005) Multi-million-year cyclic ramp-up of volatiles in a lower crustal magma reservoir trapped below the Tampakan copper-gold deposit by Mio-Pliocene crustal compression in the southern Philippines. In: *Super Porphyry Copper and Gold Deposits: A Global Perspective*, **2**. Adelaide: PGC Publishing, pp. 369–407.

Rosenbaum, G. & Mo, W. (2011). Tectonic and magmatic responses to the subduction of high bathymetric relief. *Gondwana Research* **19**, 571–582. https://doi.org/10.1016/j.gr.2010.10.007.

Rosenbaum, G., Giles, D., Saxon, M., Betts, P. G., Weinberg, R. F. & Duboz, C. (2005). Subduction of the Nazca ridge and the Inca plateau: insights into the formation of ore deposits in Peru. *Earth and Planetary Science Letters* **239**, 18–32. https://doi.org/10.1016/j.epsl.2005.08.003.

Samperton, K. M., Schoene, B., Cottle, J. M., Brenhin Keller, C., Crowley, J. L. & Schmitz, M. D. (2015). Magma emplacement, differentiation and cooling in the middle crust: integrated zircon geochronological–geochemical constraints from the Bergell intrusion, Central Alps. *Chemical Geology* **417**, 322–340. https://doi.org/10.1016/j.chemgeo.2015.10.024.

Schoene, B., Schaltegger, U., Brack, P., Latkoczy, C., Stracke, A. & Günther, D. (2012). Rates of magma differentiation and emplacement in a ballooning pluton recorded by U–Pb TIMS-TEA, Adamello batholith, Italy. *Earth and Planetary Science Letters* **355-356**, 162–173. https://doi.org/10.1016/j.epsl.2012.08.019.

Sillitoe, R. H. (2010). Porphyry copper systems. *Economic Geology* **105**, 3–41. https://doi.org/10.2113/gsecongeo.105.1.3.

Simmons, A. T., Tosdal, R. M., Wooden, J. L., Mattos, R., Concha, O., McCracken, S. & Beale, T. (2013). Punctuated magmatism associated with porphyry cu-Mo formation in the paleocene to eocene of southern Peru. *Economic Geology* **108**, 625–639. https://doi.org/10.2113/econgeo.108.4.625.

Spencer, E. T., Wilkinson, J. J., Creaser, R. A. & Seguel, J. (2015). The distribution and timing of molybdenite mineralization at the El Teniente Cu-Mo porphyry deposit, Chile. *Economic Geology* **110**, 387–421. https://doi.org/10.2113/econgeo.110.2.387.

Storck, J.-C., Wotzlaw, J.-F., Karakas, Ö., Brack, P., Gerdes, A. & Ulmer, P. (2020). Hafnium isotopic record of mantle-crust interaction

in an evolving continental magmatic system. *Earth and Planetary Science Letters* **535**, 116100. https://doi.org/10.1016/j.epsl.2020.116100.

Tatnell, L., Anenburg, M. & Loucks, R. (2023). Porphyry copper deposit formation: identifying garnet and amphibole fractionation with REE pattern curvature modeling. *Geophysical Research Letters* **50**, e2023GL103525. https://doi.org/10.1029/2023GL103525.

Toro, J. C., Ortúzar, J., Zamorano, J., Cuadra, P., Hermosilla, J. & Sprohnle, C. (2012). Protracted magmatic-hydrothermal history of the Río Blanco-Los Bronces district, Central Chile: development of world's greatest known concentration of copper. *Society of Economic Geologists Special Publication* **16**, 105–126. https://doi.org/10.5382/SP.16.05.

Turner, S. J., Langmuir, C. H., Dungan, M. A. & Escrig, S. (2017). The importance of mantle wedge heterogeneity to subduction zone magmatism and the origin of EM1. *Earth and Planetary Science Letters* **472**, 216–228. https://doi.org/10.1016/j.epsl.2017.04.051.

Ulmer, P., Kaegi, R. & Müntener, O. (2018). Experimentally derived intermediate to silica-rich arc magmas by fractional and equilibrium crystallization at 1·0 GPa: an evaluation of phase relationships, compositions, liquid lines of descent and oxygen fugacity. *Journal of Petrology* **59**, 11–58. https://doi.org/10.1093/petrology/egy017.

Warnaars, F. W., Holmgren, D. & C. & Barassi F, S. (1985). Porphyry copper and tourmaline breccias at Los Bronces-Rio Blanco, Chile. *Economic Geology* **80**, 1544–1565. https://doi.org/10.2113/gsecongeo.80.6.1544.

Weis, P., Driesner, T. & Heinrich, C. A. (2012). Porphyry-copper ore shells form at stable pressure-temperature fronts within dynamic fluid plumes. *Science* **338**, 1613–1616. https://doi.org/10.1126/science.1225009.

Wendt, I. & Carl, C. (1991). The statistical distribution of the mean squared weighted deviation. *Chemical Geology: Isotope Geoscience Section* **86**, 275–285.

Wotzlaw, J.-F., Schaltegger, U., Frick, D. A., Dungan, M. A., Gerdes, A. & Günther, D. (2013). Tracking the evolution of large-volume silicic magma reservoirs from assembly to supereruption. *Geology* **41**, 867–870. https://doi.org/10.1130/G34366.1.

Deltech Furnaces

Sustained operating temperatures to 1800° Celsius

www.deltechfurnaces.com

Gas Mixing System

An ISO 9001:2015 certified company

Custom Vertical Tube

ASME NQA-1 2008 Nuclear Quality Assurance

Standard Vertical Tube

Control systems are certified by Intertek UL508A compliant

Bottom Loading Vertical Tube